Bioactive Materials 9 (2022) 198–220

Contents lists available at ScienceDirect

Bioactive Materials

journal homepage: www.sciencedirect.com/journal/bioactive-materials

Advances in hydrogel-based vascularized tissues for tissue repair and drug screening

Ying Wang [a,b], Ranjith Kumar Kankala [c], Caiwen Ou [a,b], Aizheng Chen [c,*], Zhilu Yang [a,b,**]

[a] Affiliated Dongguan Hospital, Southern Medical University, Dongguan, Guangdong, 523059, PR China
[b] Guangdong Provincial Key Laboratory of Shock and Microcirculation, Guangzhou, Guangdong, 510080, PR China
[c] Institute of Biomaterials and Tissue Engineering, Huaqiao University, Xiamen, Fujian, 361021, PR China

ARTICLE INFO

Keywords:
Hydrogel
Vascularization
Vascular biology
Angiogenesis
Tissue regeneration
Drug screening
Vascularized tissue models

ABSTRACT

The construction of biomimetic vasculatures within the artificial tissue models or organs is highly required for conveying nutrients, oxygen, and waste products, for improving the survival of engineered tissues *in vitro*. In recent times, the remarkable progress in utilizing hydrogels and understanding vascular biology have enabled the creation of three-dimensional (3D) tissues and organs composed of highly complex vascular systems. In this review, we give an emphasis on the utilization of hydrogels and their advantages in the vascularization of tissues. Initially, the significance of vascular elements and the regeneration mechanisms of vascularization, including angiogenesis and vasculogenesis, are briefly introduced. Further, we highlight the importance and advantages of hydrogels as artificial microenvironments in fabricating vascularized tissues or organs, in terms of tunable physical properties, high similarity in physiological environments, and alternative shaping mechanisms, among others. Furthermore, we discuss the utilization of such hydrogels-based vascularized tissues in various applications, including tissue regeneration, drug screening, and organ-on-chips. Finally, we put forward the key challenges, including multifunctionalities of hydrogels, selection of suitable cell phenotype, sophisticated engineering techniques, and clinical translation behind the development of the tissues with complex vasculatures towards their future development.

1. Introduction

Tissue engineering, aiming at constructing artificial tissues *in vitro*, offers significant potential to overcome the challenges associated with the shortage of organs caused by diseases, traumas, and population aging [1,2]. The engineered tissue constructs could act as effective tools to enhance the availability of transplantation in clinical therapy and provide realistic *in vitro* models for disease modeling and drug testing [3]. However, the current research states that it is highly challenging to fabricate versatile complex tissues or organs due to the inability of the engineered constructs to systematically replicating the *in vivo* organ composition and cellular microenvironments [3,4].

Basically, the tissues and organs rely on the transportation of nutrients, removing metabolic products, and delivery of oxygen *via* densely distributed vascular networks. The lack of such diverging vascular channels within the engineered constructs has become the major fundamental obstacle that limited the applicability of the fabricated biomimetic tissue or organs using various microfabrication approaches [5]. Moreover, the limited vessels in the engineered constructs *in vitro* sometimes have shown insufficient diffusion distance (within 100–200 μm from a supply vasculature), leading to cell death and the poor lifespan of the harbored cells in the tissue constructs [1,6,7]. Thus, the availability of integrated vascular networks has become an essential criterion during the development of large, solid, and functional organs *in vitro,* mimicking the *in vivo* environment [8]. To date, the formation of vascular networks *in vitro* was firstly reported by Folkman and colleagues in 1980 [9]. The capillary endothelial cells (ECs) were cultured in a two-dimensional (2D) tumor-conditioned medium, demonstrating the development of capillary tubes. Since then, research interests in engineering the vascularized tissue constructs have been increasing [10–12].

Further efforts by various research groups have evidenced that fully

Peer review under responsibility of KeAi Communications Co., Ltd.
* Corresponding author.
** Corresponding author. Affiliated Dongguan Hospital, Southern Medical University, Dongguan, Guangdong, 523059, PR China.
E-mail addresses: azchen@hqu.edu.cn (A. Chen), zhiluyang1029@126.com (Z. Yang).

https://doi.org/10.1016/j.bioactmat.2021.07.005
Received 11 June 2021; Received in revised form 5 July 2021; Accepted 6 July 2021
Available online 10 July 2021

mimicking the physiological microenvironment in addition to the vascular networks is highly challenging as the *in vivo* conditions are too complex within native human tissues [3,4,13]. In addition, several critical issues in fabricating the well-defined constructs include the precise spatial arrangement of multiple cell types, the dynamic organizations of extracellular matrix (ECM), and complex interactions of cells within embedded ECM, requiring more in-depth research [14,15]. In general, ECM, a meshwork of polysaccharides and proteins, provides three-dimension (3D) supporting matrices simultaneously to conduct cell behavior and regulate organ functions, depending on the physiological needs during the stages of the organ analogs formation and tissue regeneration process [4,14]. The assemblies of ECM are regulated *via* reciprocate activities between various cell populations and their embedded microenvironments [16–18]. Notably, ECM mediates the crosstalk between the ECs and surrounding tissues, attributing to the retention of growth factors (GFs) in the cellular microenvironment [19,20]. These biochemical and biophysical interactions are highly dynamic within ECM surroundings, leading to the characterizations of various tissues [15,17,21]. Consequently, the biological functionalities and mechanical properties of the respective tissues determine the various ECM compositions [16,22]. Together, effective vascular networks and complex cellular environments are indispensable for vascularized tissue engineering strategy.

In tissue engineering, the designed 3D matrices based on biomaterials are regarded as an effective tool to provide a suitable microenvironment to predict cell activities, as well as orchestrate vascularized tissue formation [5,23,24]. Theoretically, the ideal scaffold materials would be the natural decellularized ECM (dECM), which could be harvested from the native tissues after acellular disposal treatment [25,26]. The predominant advantage of the dECM as scaffold materials is that it provides an integral cell growth microenvironment consisting of a variety of protein components, GFs, and other small molecules, which is essential in maintaining cell physiological functions [21,26,27]. In principle, all the potentially immunogenic components must be removed during the decellularization process while ensuring the preservation of the composition of natural ECM and raw ingredients [28,29]. However, inadequate decellularization, in some instances, may initiate strong inflammatory responses, resulting in the inhabitation of tissue remolding [25]. In addition, the content and composition of dECM obtained from different donors are varied based on similar decellularized protocols [30]. Consequently, the discontinuous decellularization and impossibility in scaling-up, along with the regulatory and ethical restrictions, restrict the therapeutic applicability of this dECM [28]. Owing to the drawbacks related to the applications of dECM scaffold materials, artificial ECM using various biomaterials has been explored over the past few years. In general, artificial ECM based on the biological scaffolds is derived from natural polymers, including polysaccharides and proteins, and synthetic matrices with biomimetic features [21,31]. Notably, it is widely acknowledged that the artificial ECM from natural polymers emerged as a promising alternative for large-scale production, manipulation, and compatibility [14,32]. In addition, multiple bioactive components, such as GFs and peptides, can be incorporated into the 3D artificial ECM, achieving the diffusion and immobilization of molecules at temporal and spatial gradients whenever necessary [19,33]. Moreover, adjustable mechanical properties and specific simulations of the tissues or organs based on artificial ECM can be achieved by varying scaffold materials [12,13,21]. However, it should be noted that the selection of biomaterials, cells, and biomolecules to reproducing the physiological conditions of the native tissue *in vitro* is critical towards the fabrication of vascularized tissue constructs, maintenance of tissue morphogenesis, as well as final achievement of organ homeostasis.

Among diverse biomaterials based on natural and synthetic origin, hydrogel materials have been demonstrated as an effective tool to serve as a 3D matrix for cells, specific factors, and drugs, attributing to their high permeability, water holding capacity, and excellent biocompatibility [34,35]. In addition to these advantages, hydrogels are often preferred over others as these soft polymeric materials resemble most of the soft tissues in the human body [36–38]. Moreover, significant advances in hydrogels have provided excellent opportunities both in engineering vascular analogs and vascularized tissues. The application of hydrogels in the human body was first reported in 1960 when Wichterle and Lim applied crosslinked poly (2-hydroxyethyl methacrylate)-based material as soft contact lens [39]. Subsequently, hydrogels were employed to encapsulate cells in 1980 [40]. Specifically, hydrogels consist of hydrophilic polymer chains embedded in a hydrated 3D environment, which allows a homogenous entrapment of multi-cell types to replicate tissue complexities [41,42]. In addition, molecules in hydrogel networks can diffuse through the interconnected pores, which satisfies the requirements of vasculature for the delivery of molecules from vessels to tissues [43,44]. Nowadays, hydrogels are widely investigated and applied for clinical therapy. To date, many researchers have reported the establishment of hollow vascular architectures based on hydrogels, ranging from micron to millimeter levels using various emerging techniques [45,46]. In addition, angiogenesis-related factors can be directly incorporated into the hydrogel to regulate the delivery of biological cues and accelerate vascular formation in the constructed tissue models. Above all, these perfusable tissue models based on hydrogels have shown great potential in modeling diverse pathological and physiological mechanisms of organs *in vitro*.

Considering the enormous potential of advanced hydrogels in engineering vascularized tissues, in this review, we first introduce the current main vascular formation mechanism, including angiogenesis and vasculogenesis. Further, the role of hydrogels in terms of physicochemical properties and intrinsic advantages is elaborately summarized towards the development of perfusable vascular architectures and subsequent vascularized tissue constructs. Finally, we discuss the applicability of these fabricated constructs in tissue transplantation, disease models for drug screening, as well as organ-on-chips (Fig. 1).

2. Regeneration mechanism of vascular networks

The vasculature is the major component of the systemic circulatory system distributed throughout the human body, branching vessels with diameters ranging from several micrometers to several millimeters (Fig. 2A) [45–47]. The arteries, compromising of hollow round channels (approximately 1 cm in diameter), branch into the smaller and thinner pipeline (100 μm −1 mm), and finally divide into a large number of capillaries (5–10 μm in diameter) for exchange of nutrients, waste products, and gases [48] (Fig. 2B). Although all the vasculatures are blood-carrying lumens, their heterogeneity in (1) physical properties, including thickness, geometries, wall components, and mechanical strength, and (2) physiological environments, including GFs, ECM compositions, and specific cell types, requires various fabrication methodologies and design criteria [47–49]. Considering the wide span of vascular diameters across several orders of magnitude and complex intertwined configurations, currently, several studies have been focused on the construction of the single-lumen structure over obtaining fully vascularized tissues to recapitulating the large vascular architecture with multiscale geometry allowing fluid flow with high pulsatile pressure [18,50,51].

To date, several advancements in developing hybrid engineering solutions and advanced fabrication techniques have been reported to enable the construction of microchannels and hollow microfibers towards imitating hollow vascular analogs [49–51]. In this vein, the human umbilical vein ECs (HUVECs) encapsulated in the hydrogel with a hollow structure showed good proliferation in culture, exhibiting a sign of the early maturation of the vessel tissue. For example, ECs within the microfibrous scaffolds migrate towards the peripheries of the microchannels to form a layer of confluent endothelium [49]. These endothelial beds were then seeded with cardiomyocytes to generate aligned endothelialized human myocardium capable of spontaneous and synchronous contraction. In addition, the wall thickness of the hollow

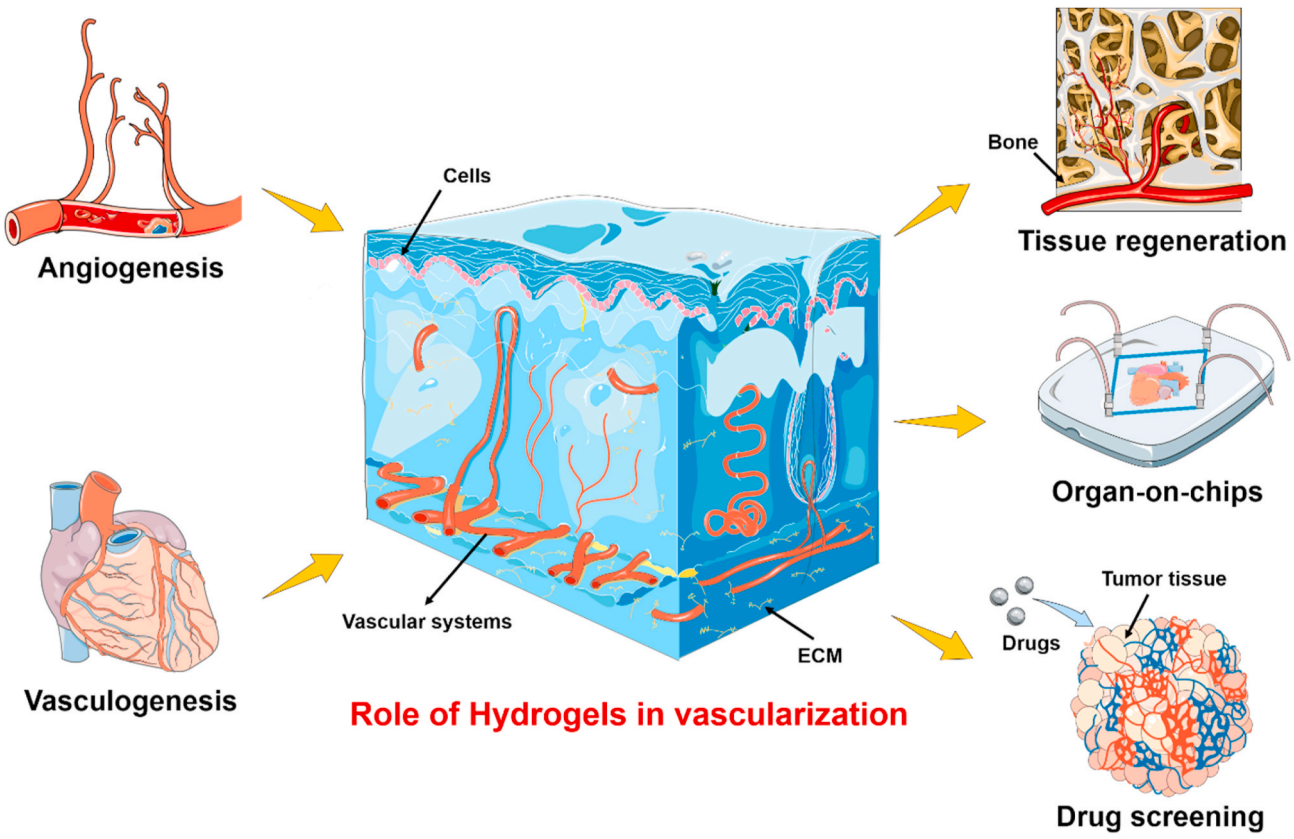

Fig. 1. Schematic illustration of the vascularized tissues in hydrogels for tissue regeneration, organ-on-chips, and drug screening. Angiogenesis and vasculogenesis mechanisms of vascular formation are introduced both in the embryo stage and postnatal life, respectively. The enrichment of the effective vascular networks enables the delivery of nutrients and waste products for the recovery of organs upon severe damage. In addition, the emerging organ-on-chips approach provides excellent opportunities for incorporating vasculatures within chips for the stimulation of physiological 3D organoids. These target 3D organoids bridge the gap between clinical trials and *in vitro* drug screening.

structures could be controlled to some extent (179.4–314.9 μm) with various gauge combinations of co-axial nozzles. Although several efforts have been dedicated to fabricating such multiscale vascular hollow architectures, there are still quite a few challenges that must be overcome to form a mature, stable, and functional endothelium within the embedded engineering tissues [50,51].

Although the perfusable vascular analogs have exhibited promising results towards the construction of various organs *in vitro*, the utilization of such biomimetic constructs in tissue regeneration upon clinical transplantation place high demands on the vascular alignment, which still remains limited for regeneration and implantation of large-scale engineered tissues, such as skeletal muscle, shin epithelium, liver, and other major organs [52–61]. Indeed, capillaries are the places where blood and tissues exchange substances, including nutrition and waste products [62,63]. However, the large-scale vessels constructed *in vitro* cannot efficiently provide nutrients like microscale capillary beds. Moreover, the ideal oxygen and nutrient delivery require a dense capillary network within 100 μm from each other, which is not feasible for surgical anastomosis [48]. To address this goal, engineered microvasculature is expected to be emphasized in mimicking the dense capillary networks and endothelial barrier functionality. In principle, the newly formed capillaries within the engineered tissue constructs can enhance the spontaneous, surgical anastomosis of microvessels [50,51,62]. However, the fabrication of capillaries, as well as vascular tree-like networks within the engineered tissues, still remains a primary challenge in regenerative medicine. Consequently, fully comprehend the mechanisms of vascular formation and physiological environment of tissue counterparts *in vivo* are extremely required during the formation of the vascularized tissue constructs *in vitro*. In this section, we introduce two primary mechanisms for improving vascularization both in the embryo stage and postnatal life, including angiogenesis and vasculogenesis, respectively. (Fig. 2C).

2.1. Angiogenesis

The angiogenesis is mainly activated by the ingrowth and sprouting of existing primitive vessels from the adjacent host tissues into the transplanted grafts, which eventually form the host-originated vessel networks [5,64,65]. In general, there are two major steps during sprouting angiogenesis, including the initial ECs growth phase and subsequently stabilization stage [66,67]. At the beginning of the ECs proliferation, the degradation and permeability of the vascular basement membrane are improved. The subsequent direction of newborn vessels is defined by the gradients of angiogenic GFs that mediates ECs migration via the signaling pathway of EC surface proteins [19,33]. In the second stabilization phase, the recruitment of smooth muscle cells (SMCs) is stimulated, leading to the maturation of blood vessels [19,33]. Considering the necessary regulation mechanism of GFs on angiogenesis, some pre-vascularization through angiogenesis strategy populated GFs into the scaffolds in order to stimulate the capillary ingrowth [68,69]. However, from the overall process, the integration of capillary formed by ECs into host vasculature is relatively slow, and the rate of angiogenesis is approximately 5–17 μm/h, during which oxygen and nutrients are usually needed [68,69]. Consequently, tedious time span and cumbersome adjustment mechanism often lead to regeneration failure and final necrosis of the organ.

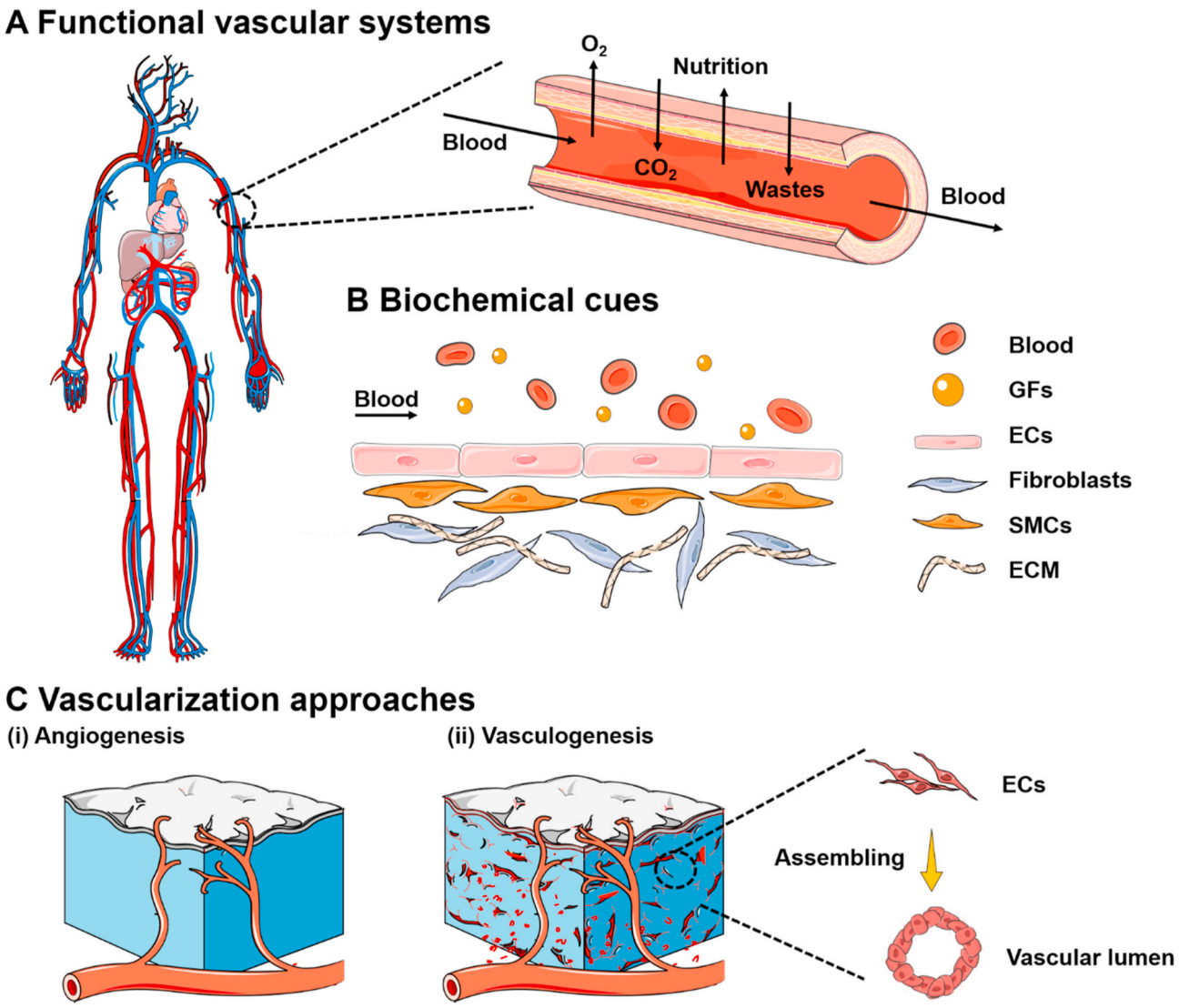

Fig. 2. (A) Schematic representation of functional vascular distribution in the human body. The vascular networks are organized into arteries (in red) and veins (in blue). The vasculatures comprise blood-carrying lumens. (B) The biochemical cues, including relevant cells and specific GFs, are expected to be integrated within the designed vascularized tissue constructs. (C) Vascularization mechanisms during (i) angiogenesis and (ii) vasculogenesis. Angiogenesis mainly relies on the sprouting of ECs to the fabricated constructs. Vasculogenesis primarily focuses on the differentiation and assembly of angioblasts and endothelial precursor cells (EPCs) into mature migrating ECs towards the repair region and subsequently forming the primitive vascular networks. (For interpretation of the references to color in this figure legend, the reader is referred to the Web version of this article.)

2.2. *Vasculogenesis*

The vasculogenesis process primarily focuses on the differentiation and assembly of angioblasts and endothelial precursor cells (EPCs) into mature migrating ECs towards the repair region and subsequently forming the primitive vascular network [70]. In the vasculogenesis strategy, ECs are always incorporated with targeted cells into the engineered hydrogel scaffolds *in vitro* to form pre-vascularization states [71–73]. In such cases, initially, the presence of ECs can stimulate the ingrowth of host vessels. Then, the formation of anastomosis of host vasculature and *in vitro* endothelial networks can be accelerated via the pre-existing endothelial networks in the engineered scaffolds [74]. Collectively, both of these strategies of angiogenesis and vasculogenesis place high requirements on the biophysical properties of scaffolds for cell delivery, biological cues transition, and perfusion with surrounding tissues.

3. Hydrogels as the artificial microenvironment

On the one hand, when designing vascular structures for large-volume blood transportation, the perfusion and structural integrity of the constructed blood vessels should be predominantly considered [50]. In this regard, the physical features of the vessels place high demands on the selection and design of suitable biological materials in terms of adjustable mechanical strength, stability of hollow structures, and orderly cell spatial distribution for the construction of perfusable vascular channels. Since vasculature is made of a single layer of ECs in native tissues, ECs are always employed to decorate the hollow biomimetic architectures, resulting in the formation of vascular analogs [75]. In this case, the hollow architectures of the scaffolds can be obtained firstly, and then the ECs are layout surrounded by the scaffold to mimic the blood vessel layer [1,45,76]. In another case, the cells can be initially distributed into the pre-solution of scaffold materials and then directly fixed in the perfusable architectures after shaping [45,50,62,77,78]. Despite the difference in the construction of blood vessels *in vitro*, the fabricated scaffolds in both instances can be utilized in

transplanting, engineering functional tissues, and understanding correlates vascular disease [7,63,79].

On the other hand, while establishing branching vascular trees within the vascularized tissues, it is required to pay more attention to the construction of the capillary beds for the transportation of nutrients [80,81]. The key strategy of creating tissue and organ constructs with vascular components plays a crucial in offering the intrinsic functionalities [3,70,74,76]. In this vein, the combination of alternative cell types, controllable shaping of architectures, and tunable biochemical cues offer the merits in engineering designed tissue or organs [69,82]. Thus, increasing the versatility of the designed scaffold materials is extremely demanding, which faces some critical challenges, such as (1) compromising vasculatures with a microenvironment that is highly similar to native ECM, (2) integrating biochemical cues inside scaffold materials to regulate cell growth, as well as tissue morphogenesis, and (3) carrying the automated process for reliable and precise fabrication of scaffolds with designed geometry and features [12,13,46].

In this section, we summarize several advantages of hydrogel-based materials in fabricating perfusable vascular microchannels and vascularized tissue constructs (Table 1). Initially, we discuss the fundamental properties and shaping mechanism of the hydrogels. In addition, we briefly summarize the advantages and disadvantages of various hydrogel gelation mechanisms in terms of their application for vascularization tissues. Further, we emphasize the physiological environments, including suitable extracellular matrix (ECM) components, relevant cell types, and proper biochemical cues to better orchestrate the superiority of hydrogel-based materials for the development of vascularized tissues *in vitro*.

3.1. Physical properties of hydrogels

3.1.1. Adequate pores within 3D hydrogel matrixes for mass transportation and molecules secretion

3.1.1.1. Tunable porous architectures for enhanced cell survival. Indeed, hydrogels provide sufficient pores within the 3D matrices which substantially facilitate the transportation of nutrients to cells and the removal of metabolic wastes within the engineered constructs [83–86]. In addition, the essential architectural parameters, including pore size, pore interconnectivity, and surface area, are tunable to a considerable extent by altering the polymer concentration, molecular weight of the polymer, and shaping techniques. In our previous work, the pore diameters of the gelatin methacrylate (GelMA) hydrogels ranged from 22.22 ± 5.57 μm to 43.47 ± 15.36 μm with varied GelMA concentration ranging from 5 to 10% (w/v) of gel solution. In addition, the proliferation of HUVECs in the GelMA hollow microfibers was observed, inducing the formation of vessel-like structures [50]. In another instance, the GelMA was crosslinked through host-guest supramolecular (HGSM), in which the crosslinking density and the pore density were increased with the increase in the HGSM content [87]. However, the pore size showed a downward trend with an increase in the concentration of the HGSM.

Compared with the usual control over the superficial pores of the hydrogel by tuning the concentration, composition, and viscosity of the pre-gel solution, the hierarchical porous structures within hydrogel constructs have been successfully developed *via* the combination of two gel systems with low interfacial energy. Notably, a fully aqueous environment ensured the biocompatible environment for cell survival and mild mass exchange with the surrounding medium. In addition, the water-in-water system offered significant advantages towards regulating pore size in a wide range without the utilization of organic solvents, cell-unfriend porogens, and surfactants. Recently, Zhang's group designed a water-in-water formulation consisting of GelMA pre-gel solution as a continuous phase and poly (ethylene oxide) (PEO) solution as a "water-porogen" [86]. The hierarchical and interconnected pores were produced in the hydrogel structures upon photocrosslinking of GelMA and further leaching of PEO droplets. Notably, the encapsulated HUVECs exhibited three- and four-fold proliferation in the porous GelMA-PEO compared to the standard GelMA. In most recent research, the hierarchically macro-micro-nano porous cell-laden hydrogels constructs were uniquely developed based on their previous water-in-water systems, which could readily recover to their initial shapes after compression [84]. These novel findings ensure that the uniquely tailored pore-forming GelMA hydrogel systems are promising candidates in further engineering vascularized tissue regeneration.

3.1.1.2. Secretion of soluble molecules from porous hydrogel matrixes. In addition to the adjustment of the morphological properties, the multicellular and soluble molecules can be secreted from porous structures following precise dose and time intervals. This mass transportation behavior between tissues and cells mainly relies on the pore size of the surrounding gel [33,86,87]. Furthermore, the biochemical cues incorporated into hydrogel matrices can be employed as biochemical regulators of cell behavior. For example, Lee and coworkers provided a localized delivery system based on the alginate gels embedding recombinant human VEGF/poly (lactic-*co*-glycolic acid) (rhVEGF/PLGA) microspheres. The prevalent release of rhVEGF promoted HUVECs proliferation substantially, thus effectively enhancing angiogenesis *in vivo* [19]. In another example, Baker and colleagues generated the temporally and spatially defined VEGF gradients within 3D gelatin/collagen gels on the microfluidic chips, guiding the location and morphology of endothelial sprouting from the channels [33]. Accordingly, controlling the morphological properties of hydrogel can effectively mimic the *in vivo* cell surroundings and thus facilitating tissue morphogenesis.

3.1.2. Wide adjustment range of mechanical properties of hydrogels to emulating the multi-native tissues

3.1.2.1. Exceptional tensile stiffness and elasticity due to the employment of hybrid hydrogel systems. The mechanical properties of hydrogel materials are essential for the construction of vascularized tissues [86–92]. On the one hand, considering the degree of stiffness in various organs, the hydrogels offer the merits to emulate the multi-native tissue from extreme stiff vascularized bone (8–17 kPa) to the utmost soft brain (0.1–1 kPa) due to the controllable mechanical strength [93]. On the other hand, the hydrogel materials can be elastic and supportive, which meets the requirement not only for maintaining the hollow channels but also withstanding the hydraulic pressure while blood flowing in terms of fabrication of vascular analogs [45,67,79,94–96]. With an in-depth understanding of hydrogel polymerization principles and crosslinking mechanisms, the hydrogel has gradually evolved from original soft and low-stretchable material towards tough and highly elastic substrates [88,89].

Collagen and elastin, extensively existing in the natural ECM, are responsible for the tensile stiffness and elastic recoil properties of the tissues, respectively [15,63,97–100]. In this vein, the engineered hydrogels derived from these natural proteins can provide exceptional strength and elasticity. Notably, the collagen-dense ECM is strictly controlled at the sub-cellular level to facilitate ECs migration during angiogenesis [98]. However, in most cases, the stiffness and other mechanical properties are still limited while using collagen or elastin solely [100]. For overcoming these deficiencies, several natural proteins or polysaccharides such as alginate, gelatin have been applied as an effective approach for enhancing the toughness and fracture energy of hydrogel [63,100]. For instance, Kim developed 3D hybrid scaffolds with outer collagen and inner alginate, exhibiting about seven times greater Young's modulus compared with the pure collagen scaffold. Furthermore, this engineered hybrid scaffold provided good granulation tissue formation and rapid vascularization between the dermis and the

Table 1
Significant hydrogel properties for vasculature.

Hydrogel composition	Cell sources	Shaping mechanism	Advantages of shaping mechanism for vascularization	Significant hydrogel properties	Advantages for vasculature	Refs.
GelMA, gelatin	HUVECs	Thermal crosslinking and photocrosslinking	Smooth gel filament extrusion at sol-gel transition and rapid UV gelation for structural support	Natural sol-gel transition of the hydrogel systems; biocompatibility; porous structure	Formation of the interconnected tubular channels within well-defined 3D architectures; a confluent endothelial layer in the inner surface of the channels; *in situ* endothelialization of the channels	[75]
Alginate, gelatin	HUVECs	Ionic crosslinking and genepin penetration	Rapidly fixation of microrods architectures and inducing HUVECs migration	Rapidly crosslinking of alginate and controllable fixation of gelatin	Unique fabrication of HUVECs-laden microrods and regulation of HUVECs migration within hydrogel microrods; formation of new capillaries and organization of intensive vascular networks in mice after injection for 21 d	[78]
GelMA, HGSM	mBMSCs	Photocrosslinking and covalently crosslinking	Enhanced mechanical properties showing self-healing capability	Synthetization of host-guest supramolecular hydrogel (HGGelMA) with high compressive strength and an excellent stretching ability; about 400% water content; 5.25-fold compression modulus of the HGGelMA (0.63 MPa) than that of pure GelMA (0.11 MPa)	Higher expression level of blood vessel-related genes (SMA, CD31, and PDGF) *in vivo* than that of pure GelMA	[87]
GelMA, PEO	HUVECs, HepG2, and NIH/3T3 cells	Photocrosslinking and leaching	The hierarchical porous structures enhancing proliferation of HUVECs	Increased Yong's modulus of the GelMA-PEO with the increase of PEO concentration	3- and 4-fold proliferation of HUVECs in the hierarchical porous GelMA than that of standard GelMA on 3 d and 7 d, respectively	[86]
GelMA, gelatin	HUVECs	Thermal crosslinking and photocrosslinking	Fabrication of pure-gelatin-based hollow structures for HUVECs encapsulation	Controllable gel point and pores diameters by adjusting gelatin and GelMA concentration, respectively	Long-term maintenance of hollow structures in culture medium	[50]
GelMA, NAGA, nanoclay	HUVECs	Photocrosslinking	Generation of a scalable large-length vascular-like microtube with variable outer and inner diameter	Marvelous mechanical properties with Young's modulus (≈21 MPa), a stretchability (≈500%), a tensile strength (≈22 MPa), an anti-fatigue performance (≈200 cycles), and a burst pressure (≈2500 mmHg)	Good permeability; formation of a complete single endothelial layer using HUVECs; the positive expression of various angiogenesis-related factors	[89]
GelMA, gelatin, HA	HUVECs, SMCs	Photocrosslinking	Spatial distribution of HUVECs and SMCs mimicking native vasculature	Adjustable tensile stress, Yong's modulus, and pore sizes	Development of heterogeneous bilayer tubular structures with HUVECs and SMCs laden on the luminal and outer surfaces, respectively	[92]
GelMA, alginate	HUVECs, DFs, and hKCs	Ionic crosslinking and photocrosslinking	Recapitulating native skin architectures by distributing HUVECs, DFBs, and KCs into three main layers	Increased compressive modulus and viscosity with an increase of alginate concentration	Higher secretion of Pro-Collα1 and lower levels of MMP-1 at 7.5% (w/v) GelMA concentration	[91]
Alginate, collagen	Keratinocyte, FBs	Cryogenic process (−30 °C)	Rapidly generation of vascular-like structures with core and shell at low temperature	Good structural stability; 7 times Young's modulus of the alginate/collagen scaffold than that of pure collagen, similar pore-structure, and cell viability	A hybrid scaffold with alginate core and collagen shell; the formation of granulation tissues and vascularization *in vivo* for 14 d	[100]
ELP	MSCs, HUVECs	Photocrosslinking	Adjustable crosslinking density mimicking stretchability of vasculature	Four times length after stretching; increased ELP concentration resulting in the increase in the crosslinking density	Maintenance of cell viabilities up to 7 d; limited cell spreading due to the lack of RGD peptide; no lymphocyte infiltration *in vivo*	[102]
PEGDA, GIA-PEGDA, RGD-PEGMA	HUVECs	Photocrosslinking	Biocompatible UV irradiation to HUVECs facilitating cell attachment	Enzymatic degradation of GIA modified PEG hydrogels; decrease in crosslinking density due to degradation	Initial HUVECs attachment at 4 h; elongation and reorganization of cells at 12 h; formation of capillary-like networks at 24 h	[80]
GelMA, PEG, SPELA	hMSCs, ECFCs	Photocrosslinking	Controllable release of angiogenic GFs using various UV curing polymers	Spatiotemporal release of BMP2 and VEGF using GF-grafted nanogel; the release kinetics of GFs depending on the PEG MW and lactide/glycolide ratio	Construction of osteogenic SPELA gel containing vasculogenic GelMA microchannels; increased vasculogenic and osteogenic differentiation of ECFCs and hMSCs	[135]
GelMA, alginate, PEGOA	hSMCs, HUCs, HUVECs	Ionic crosslinking and photocrosslinking	Direct extrusion of perfusable circumferentially multilayered tissues due to rapid ionic crosslinking	Significant increased mechanical strength compared with one or two-component hydrogels; alternative shapes and sizes without changing device	The spatial distribution of hSMCs and HUCs; creation of blood vessel tissue using hSMCs and HUVECs	[82]
GelMA	ECFCs, MSCs	Photocrosslinking	Adjustable physical properties at various UV exposure time for optimization of vascular luminal formation	Decreased degradation, increased elastic modulus, and viscous modulus with the increase of UV exposure time	Formation of ECGC-lined microvessels *in vivo* for 7 d after implantation, excessive GelMA crosslinking hindered luminal structures formation in *vivo*	[158]

Abbreviations: CD31 - platelet endothelial cell adhesion molecule-1, DFS - dermal fibroblasts, ECFCs - human endothelial colony-forming cells, ELP - elastin-like polypeptides, GelMA - gelatin methacrylate, GIA - collagen type I-derived peptide, HepG2 - human hepatocellular carcinoma cells, HGGelMA - host-guest supramolecular GelMA hydrogel, HGSM - host-guest supramolecule, hKCs - human keratinocytes, hNDFs - human neonatal dermal fibroblasts, hSMCs - human bladder smooth muscle cells, HUCs - human urothelial cells, HUVECs - human umbilical vein endothelial cells, mBMSCs - mouse marrow mesenchymal stem cells, NAGA - N-acryloyl glycinamide, NIH/3T3 - mouse embryonic fibroblasts, PEGDA - poly(ethylene glycol) diacrylate, PDGF - platelet derived growth factor, PEG - poly(ethylene glycol), PEGOA - eight-arm poly(ethylene glycol) acrylate, PEO - poly(ethylene oxide), RGD - arginine-glycine-aspartate, SF - silk fibroin, SMA - smooth muscle actin, SPELA - lactide-chain-extended star polyethylene glycol.

scaffold [100]. Moreover, regardless of hydrogel origins, researchers focused on the employment of hybrid hydrogels to improving the mechanical properties of the single hydrogel system. In a case, Eke and colleagues combined two independent networks, including GelMA and methacrylate hyaluronic acid (HAMA), to increase the compressive modulus (>6 kPa), which could be easily handled by surgical forceps without breaking [101]. In another case, Sultan and coworkers fabricated reinforced-hydrogel using GelMA and silk fibroin (SF). The increase of SF concentration resulted in an increase both in tensile stress and gelation time of the GelMA/SF hydrogels [90]. Besides, the addition of PEO into GelMA hydrogels also increased Young's modulus from 0.9 ± 0.3 to 1.4 ± 0.1 kPa, as the PEO concentration increased from 0.5% to 1.6% [86].

3.1.2.2. Tuning the strengthen by modifying the chain of hydrogel or relying on the nanomaterials. In addition to the direct entanglement of multiple polymer chains, modifying the chain of hydrogel or crosslinking sites is also practical for tuning the strength. Highly elastic and tough hydrogels could be synthesized by designing a polypeptide containing thiol residues without the incorporation of noncanonical amino acids. The crosslinking sites at the ends of the protein led to consistent molecular weight between the maintenance of excellent elastic properties of polypeptide and crosslinks. In addition, the inclusion of thiols from a pair of cysteine residues in the elastin-like polypeptide sequence allowed disulfide bond formation upon exposure to UV light [102]. As such, the engineered hydrogels showed four times the length before fracture. Rather than swelling-weaken property, most recently, liposomal membrane nanocarriers could be covalently embedded in hydrogel to regulate transmembrane transport. During the stretching process, the liposomes deformed and initiated the transmembrane diffusion of the encapsulated molecules, which trigger the formation of a new network from the preloaded precursor. In this vein, swelling-triggered self--strengthening could be achieved due to the tough nature of the double-network structure [103].

Another strategy relies on the employment of nanomaterials, such as carbon-based nanomaterials, polymeric nanoparticles, and inorganic nanoparticles to retort the mechanical properties of hydrogel scaffolds [89,104–106]. Most studies attained rigid polymer structures using these nanoparticles as physical fillers [89,104,105]. Yasmeen and colleagues demonstrated the incorporation of carbon nanotubes as nanofillers to enhance the mechanical properties of the chitosan/HA gels [104]. In another case, Shin and coworkers reported the carbon nanotube-reinforced GelMA hybrid scaffolds without affecting their porous structures [105]. These materials can either offer physical entanglement or covalent cross-linkage in the hydrogel networks [106,107]. Liang and colleagues demonstrated the physical interpenetration and covalent crosslinking between GelMA/N-acryloyl glycinamide (GelMA/NAGA) hydrogel networks and nanoclay, which could remarkably enhance the tensile strength, Yong's modulus, anti-fatigue performance, stretchability of the hydrogel, leading to the large-scale length microtubes and endothelialization of hydrogel microtubes after seeding with HUVECs [89]. In addition to the tailored mechanical performance, developing nanocomposite-based hydrogels with specific functionality, such as ion release, stimuli response, and electrical conductivity, provides enormous opportunities in developing advanced hydrogel systems [21,22,26,41,57,103,108–112]. Considering these advantages in both enhancing physical properties and facilitating cellular activities, the functional nano- or micro-composite hydrogels for engineering vascularized tissues will be further discussed in Section 3.2.3.

3.1.3. Controllable biodegradability of hydrogels for matching the rate of tissue regeneration

The degradability attribute of biomaterials in the physiological environment allows the scaffolds to gradually being absorbed and decomposed in the tissue. In some cases, a complete degradation seems not necessary, such as the regeneration of cornea and articular cartilage [17,110]. For such circumstances, the integration of native tissues and hydrogels along with a certain extent of degradation are preferred to give semi-permanent or permanent mechanical support. However, in most cases, the gradual and mild degradation of scaffold materials is required, while the poor degradation and prolonged presence of polymers at the site of transplantation sometimes may hinder the ingrowth of the native tissues [85]. Ideally, the rate of degradation is expected to match the rate of tissue regeneration. In addition, the by-product (polymer monomer and fragment) of the metabolic processes is anticipated to have a slight effect on cell survival [20,101,113].

In general, the degradation of hydrogel materials takes place mainly due to ion exchange, hydrolysis, and enzyme-induced process, along with the splitting of the 3D hydrogel networks [85]. Among others, the degradation of ECM-derived hydrogels involves enzyme induction, ECM proteins secretion, and subsequently, cells remolding, which can regulate the physiology-related processes, including cell migration, differentiation, as well as angiogenesis [16,17,25,26,55]. Although the degradation takes place physiologically and the by-products, such as glycolic acid, glucose, and lactic acid, are biocompatible, the control of degradation routing is still challenging. For example, the degradation of ionic-crosslinked hydrogels such as alginate is actually a reversed gelation process, comprising of exchange of divalent cations in alginate and eventual dissociation of ionic crosslinks, which is absolutely uncontrollable, especially in the cell culture medium containing abundant cations [59,100,114–116]. Moreover, the hydrolytic degradation process of polyethylene glycol (PEG) hydrogels from photopolymerization of poly (ethylene glycol) diacrylate (PEGDA) showed limited response to cell-secreted enzymes and cellular signals, leading to the relatively slow degradation rate both *in vitro* and *in vivo* [117]. Accordingly, considering the balance between the degradation process and tissue remolding, the degradability of hydrogels should be an alternative based on tissue demanding.

Considering these challenges, some of the synthetic hydrogels offer the merits towards the controllable degradation process due to the designed hydrolysable linkages [58,80,118]. Enzyme-sensitive peptide sequences could be incorporated into the hydrogel networks to instruct biodegradability. In a case, Zhu and colleagues reported the attachment of collagenase-sensitive GPQGIAGQ (GIA) sequence derived from collagen type I in the PEGDA chain, in which the authors observed the improved collagen sensitivity with a dependence on the concentration of collagenase [80]. Notably, the polymerized PEGDA hydrogel containing GIA and arginine-glycine-aspartate (RGD) peptides could induce the formation of capillary-like morphologies while seeding the HUVECs on the hydrogel surface, indicating that both biodegradability of scaffolds and the cell adhesion ability were essential in the organization of capillary-like networks. In another example, Hong fabricated a biomimetic adhesive hydrogel using synthetic GelMA and N-(2-aminoethyl)-4-(4-(hydroxymethyl)-2-methoxy-5-nitrosophenoxy) butanamide (NB) linked to the glycosaminoglycan (GelMA/HA-NB) hydrogel [118].

The progressive biodegradation was observed *in vivo*, in which the proportion of the implanted mass decreased from an initial 82.5 ± 5.5% at 7 d to 20.0 ± 5.0% at 56 d. Notably, the burst pressure of GelMA/HA-NB hydrogel (155 ± 27 mm Hg) was significantly higher than that of pure GelMA (31 ± 7 mm Hg), which allowed the hydrogel scaffold withstanding blood pressure. In some investigations, the adjustable biodegradation also enabled the programmed release of drugs, biomolecules, encapsulated cells, and GFs from the hydrogels, which could expand the application of hydrogel materials in tissue engineering [19,33,83,110].

3.2. Recreating physiological environments in vitro

The physiological environments of organs mainly include the relevant cell types and bioactive molecules [22,66,76,88,92,119,120]. Reproducing the appropriate physiological surroundings *in vitro* is of utmost importance to mimic the engineered constructs *in vivo*. In general, the natural ECM, comprising collagen, elastin, fibronectin/laminin, and glycoprotein, is the model for tailoring the cell-laden biomimetic scaffolds and delivery of signaling biomolecules [58,110,121,122]. Collagen and elastin primarily provide mechanical support for tissue growth [63,97,100]. In addition, fibronectin/laminin can be combined with cells and macromolecules in the ECM, which is essential in cell signaling [69,123]. The disrupted ECM equilibrium weakens the repository and regulatory effects of the extracellular space, leading to extended scar formation, as well as the loss of biological functionalities during tissue morphogenesis [16]. However, it should be noted that the understanding and simulation of the ECM components are fundamental requirements to engineer a biomimetic scaffold and display the complex multicellular interactions mimicking *in vivo*.

3.2.1. Incorporating ECM-mimetic bioactive cues

3.2.1.1. Incorporating cell adhesion peptides to improve cell-specific adhesion sites. Hydrogels provide advantages in terms of cell-specific adhesion and carrying of signal molecules due to their highly tunable linkages [19,33,117,122,124–128]. Although these hydrogels sometimes fail to offer ideal environments due to the lack of intrinsic biological activities of the natural chains such as PEG and alginate, ECM protein-derived cell adhesion peptides and angiogenic GFs can be incorporated into the hydrogel networks alternatively to overcome the inert nature and mimic ECM biological functionalities [124–126,129]. Intrinsically, the essential properties, including cell adhesion and angiogenic factors, can be applied to simulate the physiological microenvironment effectively.

To date, numerous ECM-derived bioactive peptide sequences have been incorporated into the hydrogel networks to improve cell-specific adhesion sites [117,124–126]. Among various ECM-derived bioactive peptide sequences, fibronectin-derived RGD peptide is the most commonly used one for cell-adhesive modification [117,124–126,129,130]. In addition, compared with the linear RGD sequence, the cyclic RGD can significantly improve the biological activity up to 240 times due to the enhancement of affinity to integrin $\alpha_v\beta_3$ [124–126]. Zhu and colleagues synthesized cyclic RGD peptide with a hydrophilic tail consisting of a linker of two lysine residues and a spacer of three serine residues, which could be conjugated with acryloyl-PEG-N-hydroxyl succinimide (Acr-PEG-NHS) and thus obtained cyclic RGD-PEGDA [129]. The cyclic RGD-PEGDA possessed not only excellent photopolymerization ability but also uniform distribution of cyclic RGD ligands, resulting in a significantly higher ECs population compared to the linear RGD-modified hydrogels. In another approach, GelMA, synthesized by collagen-derived gelatin and methacrylic anhydride, resembles the properties of ECM with adequate RGD motifs due to the employment of gelatin [131]. The RGD-rich property and design flexibility have made GelMA as one of the most commonly used photo-crosslinkable materials in engineering vascularized tissues, as well as tissue regeneration [50,110,111,131,132]. For instance, Chen and coworkers reported a novel aligned GelMA hydrogel scaffold for spinal cord regeneration [130]. From the platelet endothelial cell adhesion molecule-1 (CD31)-fluorescence analysis, it was observed that the density of vascular ECs in the implantation of GelMA scaffold was significantly higher than the implantation of gelatin scaffold, demonstrating a versatile method in triggering functional regeneration of the spinal cord.

3.2.1.2. Embedding angiogenic GFs within hydrogel matrices. GFs, ascribing to various polypeptides, transmit signals to modulate cellular activities via specific binding to the receptors on the surface of the target cells (Table 2) [19,33,127,133]. Since the dosage response, addition time, and gradient profile of GFs are extremely crucial for inducing cellular function and tissue revolution, the persistent stimulation with a fitting level of GFs is still an issue that needed to be resolved for the development of functional vascularized tissues *in vitro* [6,19,20,97,127,134]. Numerous attempts have been made in encapsulation the GFs into hydrogel matrixes through physical interactions (adsorption and complexation) [97], covalently attaching [134], and chemical modification by heparin due to the short half-lives in free forms [122,128]. In addition, the combined effects of multiple GFs other than individual GF have been widely investigated based on hydrogel systems [19,135,136]. These bioactive cues released from the scaffolds can facilitate rapid infiltration of host blood vessels. For example, the spatial and time-release of VEGF and bone morphogenetic protein-2 (BMP-2) was achieved *via* VEGF-grafted nanogels and BMP2-grafted nanogels [135]. Interestingly, the secretion of VEGF and BMP-2 from nanogels was independent of the protein size but dependent on the length of the degradable segment. In addition, BMP2-grafted nanogels and human marrow mesenchymal stem cells (hMSCs) were encapsulated in the lactide-chain-extended star polyethylene glycol (SPELA) hydrogel. VEGF-grafted nanogels, hMSCs, and ECFCs were encapsulated in GelMA hydrogel. The osteoblast-vascular niche was developed *via* embedding GelMA microchannels into the SPELA patterned hydrogel matrix. In another instance, three kinds of GFs, including VEGF, PDGF, and SDF-1, were secreted from hypoxia-inducible factor-1α (HIF-α)-mutated muscle-derived stem cells (MDSCs) to accelerate vascular ingrowth and neovascularization within heparin-coated GelMA/HAMA hydrogel

Table 2
Main GFs involved in the regeneration of vascular networks.

GFs	Main function	Ref.
VEGF	The key regulator of angiogenesis during embryogenesis; promoting ECs migration, proliferation, vascular permeability, and degeneration of ECM through binding to the receptors with tyrosine kinase activity	[200, 201]
bFGF	Inducing plasminogen activator and collagenase activity; a strong synergistic action with VEGF accelerating ECs migration	[202]
PDGF-B	Stabilizing and enclosing the channels of ECs, leading to the maturation of blood vessels	[203]
ANG-1	Maintaining the interaction between ECs and surrounding supporting cells and the stability of blood vessel structure	[184]

Abbreviations: ANG-1 - angiopoietin-1, bFGF - basic fibroblast growth factors, GFs - growth factors, PDGF-B - platelet-derived GF-B, VEGF - vascular endothelial growth factors.

scaffold [136]. Subsequently, the constructed GelMA/HAMA hydrogel scaffold was then implanted within mice to repair the injured cavernosum, demonstrating vascularization in cavernosa and repair of cavernous defects. Above all, the cooperation of multiple angiogenic factors holds great promise for engineering vascularized tissue and tissue regeneration.

3.2.2. Incorporation of multiple cell types

3.2.2.1. Involvement of proper ECs subtypes. The cell types, including the selection of proper ECs (HUVECs; human microvascular ECs, HMVECs; endothelial progenitor cells, EPCs; and embryonic stem cells, ESCs) and involvement of multiple supporting cells (pericytes; vascular SMCs, VSMCs; and FBs) for engineering vascularized tissue constructs *in vitro* must be considered carefully to maintain their growth effectively, thus guiding the vascularized tissue formation [133]. In terms of arteries or large blood vessels, vasculature is made of a single sheet of ECs that are tightly arranged on the interior surface of blood vessels. The ECs layer is then surrounded by one or more layers of VSMCs or connective cells, which finally be embedded into the connective tissues [94,123,137]. However, capillaries only consist of a single sheet of flattened ECs and scattered pericytes [94]. Moreover, in different organs, endothelium exhibits various architectures, molecular signatures, and barrier functions in tissue-specific phenotypic heterogeneity [138]. For instance, abundant neovascularization is desired in the injured tissues for supplying oxygen and nutrients, which could improve the regeneration effect following the damage. On the contrary, the dysregulated vasculatures may lead to serious pathogenesis, such as the most typical disease, cancer. Accordingly, the selection of different phenotypes of ECs and supporting cells needs to be considered carefully when designing the models of vascularized constructs [91].

In this vein, a wide variety of ECs subtypes are currently available, ranging from primary isolated ECs to cells differentiated from progenitor or stem cell populations. Among others, HUVECs remain the most prevalent choice due to the relatively easy accessibility and alleviation of immune rejection [78,126,139]. Notably, HUVECs specifically express vascular endothelial cadherin (VE-Cad) and CD31, which is helpful in effectively identify them as ECs [78,107,130]. In our previous study, CD31 and VE-Cad staining were operated both *in vitro* and *in vivo*, indicating the growth, maturation, and organization of HUVECs [23,78]. Similarly, EPCs, showing the possibility of differentiating into mature functional ECs, are characterized by the expression of hematopoietic progenitor cell antigen (CD34) and vascular endothelial growth factor receptor-2 (VEGFR-2) markers [140,141]. Moreover, the origins of EPCs (bone marrow, peripheral blood, and lipoaspirate tissue) make them prefer clinically relevant cell sources for engineering intra-organ vascular trees. HMVECs, varying in phenotype and morphology based on cell sources (dermal, lung, and uterine tissues), are suitable for tissue-specific vascularization, especially for the study on angiogenesis in the tumor microenvironment [142].

3.2.2.2. Supporting cells guiding the vascularized tissue formation using hydrogels. In addition to the proper ECs, various supporting cells should also be considered to sustain ECs growth [15,17,91,139,143]. For the construction of large blood vessels, SMCs act as vasodilators and vasoconstrictors, which help altering vascular mechanical strain and pulsatile flow of blood [82,92,139]. For instance, Bak and colleagues cocultured SMCs and HUVECs within thermo-responsive hydrogels [133]. Not only the VEGF expression was up-regulated in the coculture group, but also the tube length of capillaries and the number of arterioles were significantly increased after implantation for 4 weeks in mice compared with the injection of HUVECs or SMCs only. FBs are another type of vital supporting cells specifically for synthesizing and maintaining the ECM by secreting collagen [15,17,91]. Blinder and colleagues reported the coculture of HUVECs and neonatal human dermal FBs in a fibrin-based scaffold and showed the dynamics of neovascular formation [69]. Notably, the vascular morphogenesis was time-correlated with the deposition of an ECM-rich environment. In another example, Whisler and coworkers seeded HUVECs in fibrin gels and cultured them alongside human lung FBs within a perfusable microfluidic platform [123]. Interestingly, the sprouting vessels could maintain a stable morphology with the presence of FBs, while the nascent EC networks would rapidly degenerate without coculture of FBs, indicating the communications and interactions between HUVECs and FBs. Furthermore, the organ-specific supporting cells are varied among organs. Depending on the *in vivo* counterparts to be simulated, the selection of unique supporting cells should be considered to enhance the integration between the vascularized constructs or engineered vessels to the host vasculatures [1,3,28,52,76,94,144]. For instance, chondrocytes provide major supporting systems to facilitate cartilage formation in the bone tissue environment [145,146]. The blood-brain barrier depends on the extensive presence of pericytes and astrocytes [94,147]. Together, both the selection of ECs and coculture of ECs with supporting cells play vital roles in engineering vascularized tissue constructs and various organs.

3.2.3. Incorporation of tailored micro-, and nanomaterials in response to the demanding for cellular signals

Since the growth of the vessel is an integral process involving numerous cues and GFs, the cooperation of various biometric signals into the engineered scaffolds can significantly govern the formation of vascular networks and effectively enhance the feasibility of vascularized tissues *in vitro* [22]. Hydrogels have been widely investigated as carriers of various hydrophobic or hydrophilic molecular cargos to target sites or injured tissues by releasing these biological cues in a programmed manner towards improving the angiogenesis process [6,19,97]. Initially, this conventional approach was applied to employing the hydrogels with different degradation rates as the desired sequential release platforms. However, these GF-supplemented scaffolds were troubled by the initial burst release of molecules from the hydrogel matrixes [148]. To overcome this challenge, the angiogenic factor-encapsulated polymeric particles were integrated within the hydrogel matrixes. For instance, Yonet-Tanyeri developed a non-degradable poly (ethylene glycol) dimethacrylate (PEGDMA) hydrogel patch, compromising VEGF121-contained poly (ethylene imine) (PEI)-PEGDA gel and VEGF165-laden PLGA microparticles (Fig. 3A) [149]. Initially, the PEI-PEGDA (Fig. 3A–i) could rapidly degrade due to cleavage of amino ester linkages between PEGDA and PEI (Fig. 3A–ii), leading to the immediate release of VEGF121 under degradation. Further, the VEGF165 was released from PLGA microparticles in a sustained fashion and then escaped from the PEGDMA patch (Fig. 3A–iii). Consequently, the sequential release of dual VEGF isoforms was achieved, demonstrating a more effective promotion of vascular sprouting and size expansion than releasing dual VEGF isoforms simultaneously or singular VEGF release (Fig. 3A–iv and v).

In response to the demanding for various cellular signals in engineering tissue or organs *in vitro*, the focus of the researchers has been gradually shifted in recent times towards the development of composite gel systems using nanomaterials for the intended molecular delivery. These nanocomponents can physically or covalently be incorporated within the hydrogel bulk, leading to the nanocomposite hydrogel networks with exceptional physicochemical properties [106,107]. Moreover, the filler micro-and nanomaterials sometimes supply additional functionality, such as the promotion of electrical conductivity and facilitating tissue regeneration. As reported, a wide range of particulate forms, including inorganic nanoparticles, carbon-based nanomaterials, and metal nanoparticles, are combined to obtain such nanocomposite hydrogels [105,112,150,151]. In an example, the conductivity of electrical-conductive hydrogel using chemically reduced GO/GelMA (rGO/GelMA) was significantly higher than that of unreduced GO-incorporated GelMA (GO/GelMA) [106]. The incorporation of

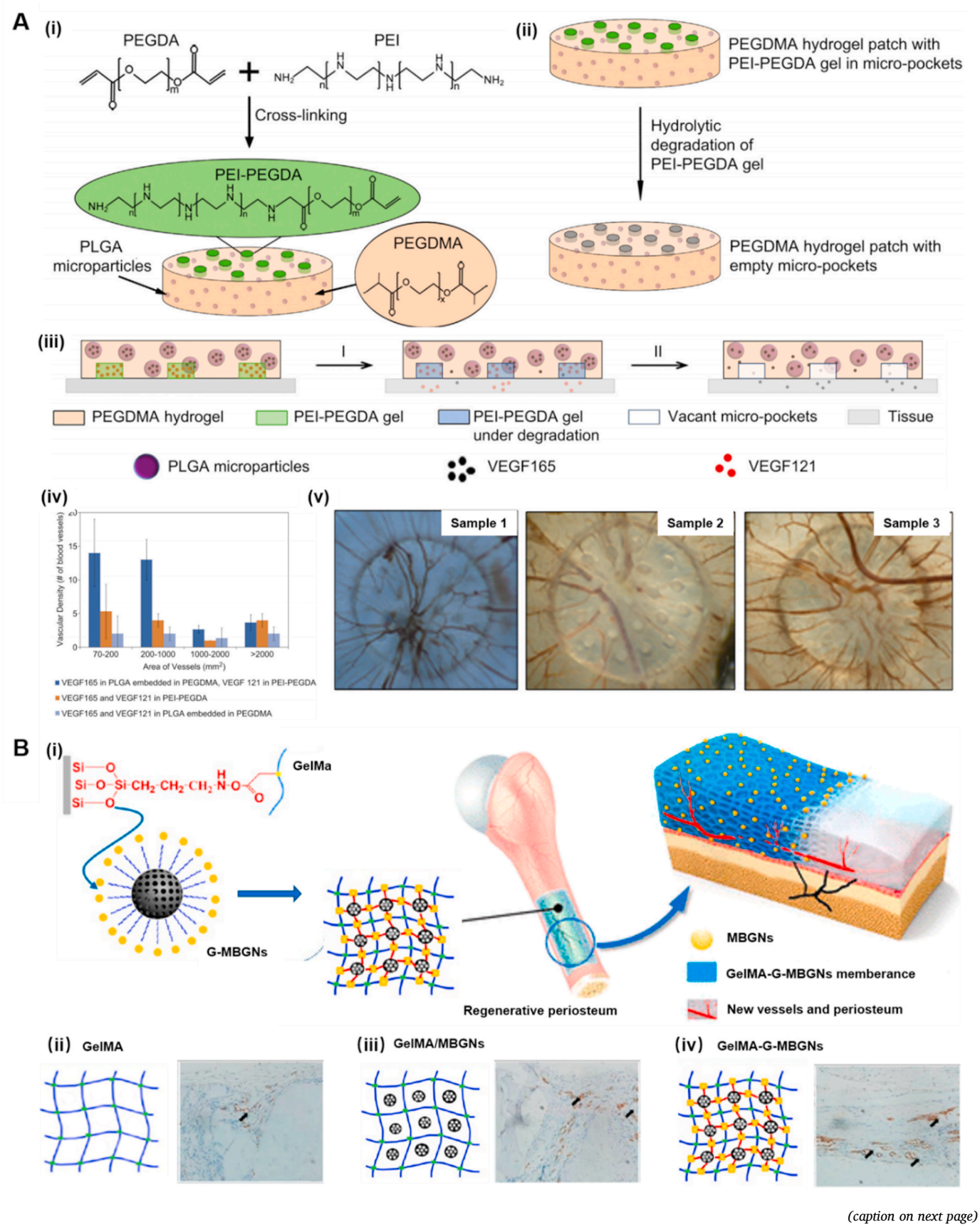

(caption on next page)

Fig. 3. The design and application of (A) nanocomposite hydrogels and (B) micro composite hydrogels for angiogenesis and vasculogenesis. (A) Schematic illustration of the PEGDMA hydrogel patch (orange) in which PEI-PEGDA gels (green) are loaded in multiple micro-pockets and PLGA microparticles (violet) are embedded. (i) Representation of the chemical structure, (ii) bimodal hydrolytic degradation of the PEGDMA hydrogel patch, (iii) mechanism of the sequential molecular release from the PEGDMA hydrogel patch. Rapid VEGF121 (red) release with the degradation of the PEI-PEGDA gel and sustained VEGF165 (black) release from the PLGA microparticles, (iv) Quantified vascular density of chorioallantoic membrane (CAM), and (v) top view of the vasculature of CAM implanted with hydrogel patches. Sample 1 is the CAM implanted with a patch in which VEGF121 was loaded in the PEI-PEGDA gel, and VEGF165 was encapsulated in the PLGA particles embedded in the PEGDMA hydrogel. Sample 2 is the CAM implanted with the gel patch in which VEGF121 and VEGF165 were loaded in the PEI-PEGDA gel. Sample 3 is the CAM implanted with the gel patch in which VEGF121 and VEGF165 were loaded into the PEGDMA hydrogel. Reprinted with permission from Ref. [149]. Copyright 2013, Elsevier. (B) Inorganic strengthened hydrogel membrane for regenerative periosteum along with new vessels sprouting. (i) Fabricating amino-modified MBGNs and GelMA-MBGNs (G-MBGNs), (ii) pure GelMA and staining of CD31 at 8-week post-implantation, (iii) preparing GelMA/MBGNs and staining of CD31 at 8-week post-implantation, and (iv) preparing GelMA-G-MBGNs and staining of CD31 at 8-week post-implantation. The arrows indicate the new blood vessels. Reprinted with permission from Ref. [107]. Copyright 2017, America Chemical Society. (For interpretation of the references to color in this figure legend, the reader is referred to the Web version of this article.)

superparamagnetic iron oxide nanoparticles (SPIONs) in the star-shaped PEG with acrylate end groups could induce an ultrahigh magnetic response [151]. Silver nanoparticles enclosed into soft GelMA gels could accelerate wounding healing [111]. Conclusively, the employment of designed micro- or nano-materials is helpful in further expanding the applications of hydrogel systems in regenerating vascularized tissues.

3.3. Alternative hydrogel formation mechanisms

In most cases, cells are encapsulated into the hydrogels to develop tissues or organs in order to form a complex 3D culture environment [40,90]. Accordingly, the gelation processes and hydrogel solutions must be biocompatible. A variety of polymers, including natural and synthetic origins, can assemble of a liquid monomeric phase and be processed into hydrogels through self-assembly, thermos-condensation, chemical, and ultraviolet (UV)-irradiated photocrosslinking approaches, which appears the great versatility in physicochemical properties and gelation approaches of the hydrogel systems [152–154]. However, each shaping mechanism provides unique advantages and respective disadvantages towards the application of tissue engineering. Among others, the physical gelation approaches, such as thermo-response entanglement, are easy to achieve and reverse along with the limited tunable properties of hydrogels [83,108,113,133,155,156]. As for the prevalent chelation interactions, alginate is a prominent example to rapidly gel in the presence of divalent cations [59,100,114–116,119]. The clipping process can occur in well-defined spaces, which facilitates the formation of distinctive tissue structures [78]. However, the lack of specific cell-binding motifs or receptors limits the enzymatic degradation of alginate under physiological conditions. In addition, potential calcium-related toxicities sometimes hamper the utilization of alginate [85,115,116]. Accordingly, in some cases, the removal of the alginate component was considered after gel shaping [137].

In recent years, UV-irradiation has been extensively used to initiate crosslinking [101,154,157]. During the shaping process of hydrogel, the mixed photo-initiators within hydrogel systems are excited by UV to create free radicals, which further interact with photo-curable macromers to stimulate crosslinking in the 3D polymeric networks [154]. Although the photocrosslinking approach has been widely utilized in building hydrogel systems, photoinitiation based on the presence of photo-initiators can lead to unforeseen toxicity issues to encapsulated cells [157,158]. In addition, the exposure time to UV light can affect the crosslinking density and thereby disturbing cell behavior. For example, Lin injected the GelMA solution containing human ECFCs and mesenchymal stem cells (MSCs) into mice to explore the effect of the degree of GelMA crosslinking to neovascularization *in vivo* [158]. They demonstrated that the cell spreading was progressively diminished by increasing the UV exposure time from 15 to 45 s. In addition, the cell viability was negatively affected beyond 300 s under UV exposure. Notably, they examined the application of UV light to modulate vascular morphogenesis in mice. The number of perfused blood vessels was significantly decreased from 374.7 ± 174.2 lumens mm^{-2} using 15 s UV exposure time to 145.1 ± 105.5 lumens mm^{-2} using 30 s UV exposure time, while no obvious blood vessels were observed in the GelMA hydrogels after 45 s exposure. Moreover, the morphology and lumen geometry of newly formed vessels were also larger using 15 s of UV irradiation (96.12 ± 10.5 mm^2) compared with 30 s of irradiation (39.1 ± 5.3 mm^2). In consideration of the benefits and limitations of various shaping approaches above, currently, several reports presented the integration of multiple hydrogel components and shaping mechanisms to enhance the physicochemical properties of the hydrogels [152,154]. Basically, the physical properties, such as viscosities of hydrogel aqueous solutions, swelling abilities, and mechanical properties after shaping, can be altered to some extent [100,116]. Furthermore, these multifunctional features of hydrogels also provide excellent opportunities for manipulating these hydrogels on various engineering techniques, including 3D printing, microfluidic spinning, and co-coaxial extrusion technology [159–161].

Nowadays, the majority of the combined gelation approaches rely on the combination of UV photocrosslinking with thermo-crosslinking or ion-crosslinking [50,78,132,162]. On the one hand, as for the thermo-crosslinking, thermal responsive polymers are directly entangled into the hybrid hydrogel solutions, and the most prevalent one is collagen-derived gelatin [50,132]. During the gelation process, successive reversible physical entanglement and the irreversible photocrosslinking of the hydrogel systems can be achieved (Fig. 4A) [132]. In the first step, the GelMA/gelatin bioinks were rapidly held under the gel point of gelatin, and in the second step, the gelatin was dissolved away after further stabilized by photocrosslinking without change of the scaffold geometry (Fig. 4B). Consequently, the blend of gelatin with GelMA could avoid the irregular filament shapes, time-consuming shaping process, and inadequate mechanical strength after printing at low GelMA concentration [132]. Notably, this blending hydrogel system based on gelatin could also cater to the microfluidic-based coaxial nozzle devices (Fig. 4C) [50]. In addition, the encapsulated HUVECs in the GelMA/gelatin gel exhibited excellent viability. The hollow structures of the constructed GelMA/gelatin microfibers were similar to blood vessels which could also be maintained after 10 d of cell culture. In addition to the natural polymers, the synthetic macromolecules, such as poly (N-isopropylacrylamide) (PNIPAAM) and polyacrylic acid (PAA), are also thermal responsive that can be utilized in vascularized tissue engineering [83,113,133,155].

On the other hand, alginate is another universally applied polymer for spontaneous physical gelation based on the chelation of polycarboxylates with Ca^{2+} or other divalent metal ions [59,100,114–116,119]. Commonly, the gel formation takes place rapidly when the alginate contacts with calcium ions, leading to the precisely controlled anisotropic architectures and possibilities to prepare scaffolds of various shapes such as microrods [78], hollow microfibers [96], and helical structures [114]. In general, in the fabrication systems, the ionic solution of calcium ions and an aqueous solution of alginate were induced in dual syringe needles that were connected to the applicator, separately (Fig. 4D) [49]. During the bioprinting process, the bioink was extruded without clogging, following the firstly ionic crosslinking of the alginate component, and secondly, crosslinking of GelMA by UV exposure. In

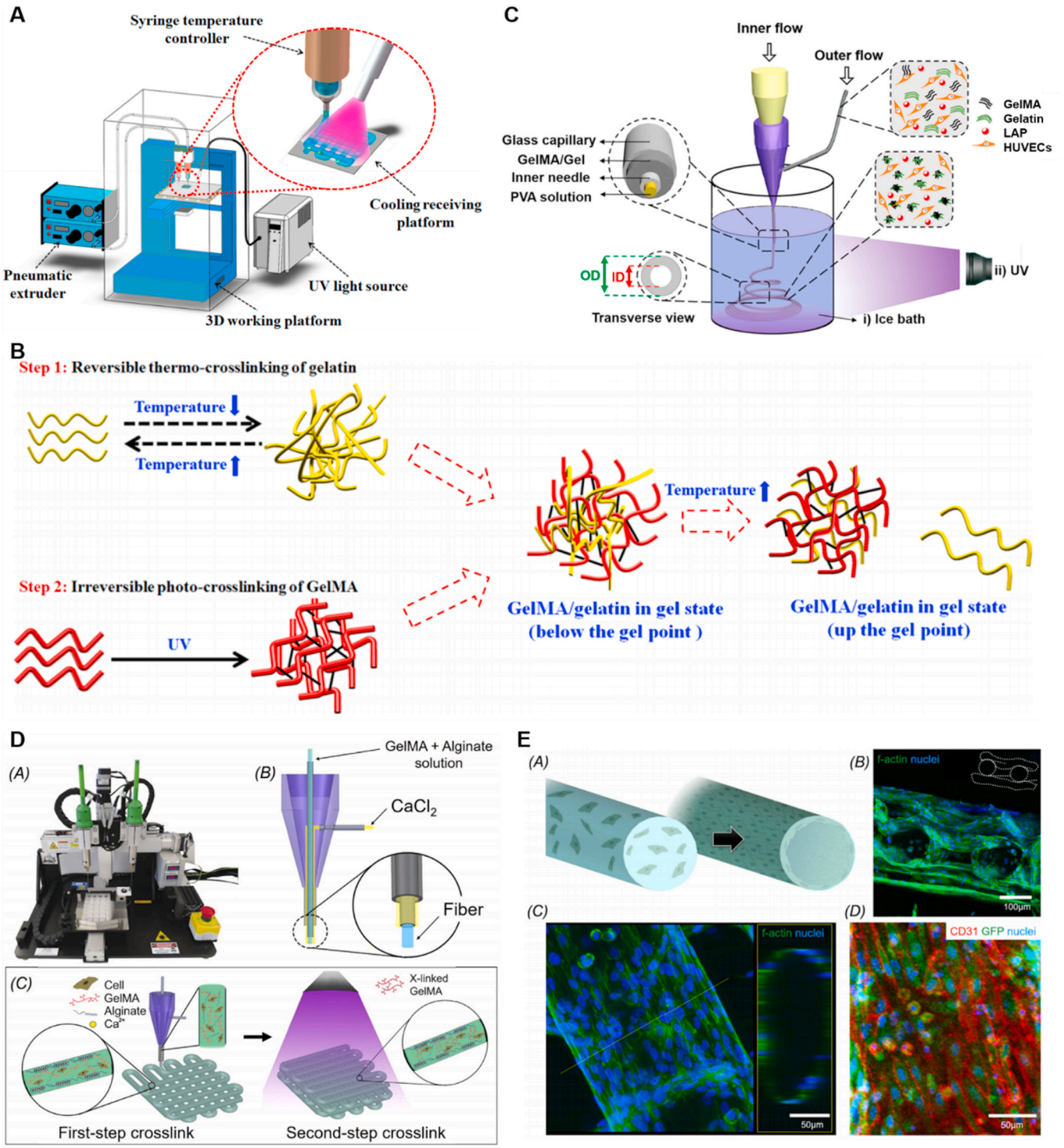

Fig. 4. (A) Schematic of the 3D bioprinting system: the temperature controller on the syringe regulated the viscosity of GelMA/gelatin bioinks; the cooling system under the receiving platform temporarily thermo-cross-linked gelatin in the bioinks; and the UV light permanently photo-crosslinked GelMA in the bioinks. (B) Two-step cross-linking of GelMA/gelatin bioinks. Reprinted with permission from Ref. [132]. Copyright 2018, ACS. (C) Schematic illustrating the setup for generating hollow GelMA/Gel microfibers by microfluidic coaxial biofabrication for cannular tissue engineering. Reprinted with permission from Ref. [50]. Copyright 2019, ACS. (D) Photograph of an Organovo bioprinter. Schematic of the coaxial needle where the bioink is delivered from the core and the ionic crosslinking $CaCl_2$ solution is sheathed on the side. Schematic diagrams showing the two-step crosslinking process, where the alginate component is first physically crosslinked by the $CaCl_2$ followed by chemical crosslinking of the GelMA component using UV illumination. Reprinted with permission from Ref. [49]. Copyright 2016, Elsevier.

addition, the ECs could be encapsulated into the alginate/GelMA hydrogel to generate a perfusable vascular template after immigration (Fig. 4E). Accordingly, the alternative hydrogel formation approaches are significant to enhance manipulation flexibility.

4. Potential applications

An impressive spectrum of cell biology, versatile hydrogels, and clinical pathology has enabled the formation of 3D tissue analogs with promoted vascularization. To date, an extensive study has demonstrated

various organ types that can be mimicked by hydrogels, including but not limited to bone [77,95,163–165], kidney [52–54], liver [55–57], lung [160,166,167], muscle [58–61], and brain [138,168]. Ultimately, the generation of these reproducible and accurate 3D organoids has extended the downstream translational applications, including tissue regeneration (Table 3), organ-on-chips (Table 4), and drug screening (Table 5). In this section, initially, we discuss the transplantation or injection of the vascularized organoids engineered by hydrogels for tissue repair. We further discuss the current applications of the hydrogel in organ-on-chips and drug development.

4.1. Tissue regeneration in vivo

Although some tissue repairs and organ regeneration can be accomplished relying on the self-repair pathway to some extent, the recovery of organs is usually overlooked upon severe damage due to the lack of vascular networks remolding in the defect area [11,17,106]. Currently, organ-failure or tissue-loss patients severely suffer from donor organ deficiency, invoking the construction of the vascularized tissues for tissue regeneration [157]. From the perspective of tissue-engineering-approach, the effective strategies for tissue regeneration *in vivo* are mainly divided into two categories. An obvious and first strategy that should be considered directly is tissue transplantation [19,33,95,96,163,165]. The other effective approach that should be realized is the employment of the injectable vascularized microtissues for *in situ* tissue regeneration [19,84,85,104,121,151,160,169–172].

Understanding the regeneration process and biological mechanism provide opportunities for the restoration of the damaged tissues. Most early studies relied on the host vessel infiltration to support graft survival in the third regeneration phase [150,173]. However, this angiogenesis process sometimes is too slow to form sufficient newly-born capillaries upon severe damage, leading to the final tissue necrosis [173,174]. More recently, the implantation of pre-vascularized constructs showed great potentials in facilitating the anastomosis of the host vessels and the *in vitro* formed vascular networks [11,12,30,95,165] (Fig. 5A). Taking the most common bone repair as an example (Fig. 5B), in general, the repair process can be broadly classified into the following overlapping steps after the formation of the bone fracture (Fig. 5B–i): the initial inflammatory phase (Fig. 5B–ii), in which the inflammatory cells infiltrate the injured site, leading to the formation of granulation tissue and migration of mesenchymal cells; (ii) the subsequent regeneration phase (Fig. 5B–iii), in which collagen matrixes are deposited, and osteoid is secreted to form a soft callus at the injured site, along with the ingrowth of vascular networks; (iii) the final tissue maturation (Fig. 5B–iv), involving ECM remodeling and the balance between the functional achievement or scar formation [11,30,70,170].

Basically, the cooperating of the relevant vascular cell sources or GFs is the most direct way to promote vascularization *in vitro*. In an example,

Table 3
Construction of various organs with specific vascular morphology by hydrogel and its application in tissue regeneration.

Hydrogel types	Cell sources	Organoid types	Vascular morphology/signals	Significant advantages of hydrogels	Major results	Ref.
GelMA, HAMA	HIF-1α mutated MDSCs	Corpus cavernosa	Ingrowth of vascularized tissue ingrowth and promotion of neovascularization	Similar multi-scale porous structure and Yong's modulus of hydrogel scaffolds to native corpus cavernosum	Heparin coating and secretion of VEGF, PDGF, and SDF-1 from MDSCs; restoration of the erectile and ejaculation function	[136]
GelMA	HDFs, HUVECs	Skin flap	Formation of HUVEC- tubes; increased density of microvessels *in vivo*	Controllable mechanical and degradation properties	Supporting for HUVECs proliferation and migration; a rapid formation of HUVEC-tubes	[157]
GelMA, gelatin	BMSCs	Spinal cord	Increased number of vascular ECs *in vivo* quantified by CD31 and synaptophysin staining	High elasticity and water content of the hydrogel scaffold	promotion of differentiation of BMSCs into neurons; formation of glial scar	[130]
GelMA, MBGNs	MC3T3-E1	Periosteum	Formation of the initial circular lumen and further regular annular lumen by ECs after surgery for 4 and 8 weeks, respectively	Prolonged ion release, better mechanical strength, and more durable degradation time compared to pure GelMA	Fabrication of GelMA/MBGNs by physically mixture and GelMA-G-MBGNs by chemically modification, separately; quantified neovascularization GelMA-GMBGNs group > GelMA/MBGNs group > GelMA group > blank group at the same time after implantation	[107]
GelMA	BMSCs	Endochondral bone	GelMA architectures with interconnected microchannels in a diameter ranging from 265 to 1225 μm	Easy manipulating hydrogel architectures with hollow microchannels	Intensive vascular networks; enhanced vascularization within core regions of the microchannel GelMA templates; promotion of osteoclast/immune cell invasive and vascularization upon implantation	[95]
HAMA, GelMA	HUVECs, ADMSCs	Bone	Complex capillary-like networks *in vitro*; increased vessel density and area distribution of microvessels *in vivo*	Bioactive hybrid hydrogel solutions for differentiation of stem cells	Co-culture of HUVECs and ADMSCs within hydrogel coating improved vascularization *in vitro*, along with no significant effects on osteogenesis; functional anastomosis of capillaries in scaffold with the host vasculature	[163]
GelMA	HUVECs, hMSCs	Bone	500 μm hollow channels within hard PLA scaffold; formation of capillary-like and lumen-like structures within biphasic constructs	Formation of biphasic constructs using hydrogel and delivery of angiogenic GFs within hydrogel matrixes	The formation of rounded morphologies of encapsulated cells within GelMA; enhanced osteogenic differentiation and vascularization due to the presence of BMP-2 peptide and VEGF peptide	[165]
Alginate, ceramic ink	HUVECs	Bone	Existing of about 500 μm hollow pipe in the middle of the strut	The regulation of HUVECs migration by ionic products *in vitro*	Promotion of bone marrow formation and bone marrow cavity reconnection	[96]
Alginate, gelatin	BMSCs	Bone	The positive expression of CD31 after injection for 3 weeks	Increased pore size with the increase of Mg particles within hydrogel	Development of *in situ* pore-forming injectable hydrogels	[85]

Abbreviations: ADMSCs - adipose-derived mesenchymal stem cells, BMP-2 - bone morphogenetic protein-2, BMSCs - bone marrow mesenchymal stem cells, CD31 - platelet endothelial cell adhesion molecule-1, GelMA - gelatin methacrylate, GFs - growth factors, HAMA - methacrylate hyaluronic acid, HDFs - human dermal fibroblasts, hMSCs - human marrow mesenchymal stem cells, HUVECs - human umbilical vein endothelial cells, MC3T3-E1 - mouse embryonic osteoblasts precursor cells, MDSCs - muscle-derived stem cells, PDGF - platelet derived growth factor, VEGF- vascular endothelial growth factors.

Table 4
Angiogenesis/vasculogenesis on-a-chip.

Hydrogel types	Cell sources	Organoid types	Vascular morphology/signals	Major results	Ref.
Fibrin	HUVECs, lung FBs	Microvascular	Complex perfusable microvascular networks	Diseased vessel diameter by adding VEGF or increasing fibrinogen concentration	[123]
Fibrin	HUVECs, lung FBs, pericytes, hGMCs	Complex angiogenic sprouts and primary vessel network.	Spatially controlled co-culture of HUVECs with different cell types	Interconnected vasculogenic networks due to the co-culture of lung FBs; formation of a gradient of LF-secreted factors to induce angiogenic sprouting; simulation pericyte recruitment from interstitial tissue; mimicking of tumor vasculatures	[181]
Fibrin	HUVECs, hMSCs	Microvascular networks	Calculation of the size of microvascular networks, average vessel diameters, and length of branches for HUVECs only and co-culture condition	Generation of a non-interconnected microvasculature with the addition of TGF-β1; promotion of functional networks with the addition of Ang-1; reduction of mean vessel diameter and increased number of network branches with the presence of mural cells	[184]
Gelatin, fibrin	HUVECs, hMSCs, hNDFs	Osteogenic differentiation	HUVEC-lined vascular channel	The viability of hNDFs decreased at distance more than 1 mm from the embedded vasculature; differentiation of hMSCs to an osteogenic lineage	[186]
Collagen	HUVECs, NIH/3T3	Vasculature	The confluent monolayers within the channels about 200 μm	Two endothelialized tubules within a stromal compartment; generation of spatially defined VEGF, bFGF, and phorbol myristate acetate gradients; investigations of invasion depth and sprouting morphology induced by GF gradients	[33]
PEGMA, PEGDA, GelMA, SPELA	HUVECs, MC3T3	Microchannel networks	150–1000 μm diameters of microchannel using various dispensing capillaries	Enhanced mass transport, differentiation, cellular viability within the constructs due to the presence of GelMA; proliferation of HUVECs at high GelMA concentration.	[187]
Collagen, gelatin	HUVECs, C2C12 cells	Vascularized muscle bundle	Microchannel at 500 μm in diameter	Formation of robust HUVEC-junction in 24 h; immediate HUVEC-sprouting with a muscle fiber; longer length of vessel sprouting in vascularized muscle bundle compared with the group without muscle bindle.	[188]

Abbreviations: bFGF - basic fibroblast growth factors, C2C12 cells - mouse myoblasts, FBs - fibroblasts, GelMA - gelatin methacrylate, hGMCs - human glioblastoma multiforme cells, hMSCs - human marrow mesenchymal stem cells, hNDFs - human neonatal dermal fibroblasts, HUVECs - human umbilical vein endothelial cells, MC3T3 - mouse embryonic osteoblasts precursor cells, NIH/3T3 - mouse embryonic fibroblasts, PEGDA - poly(ethylene glycol) diacrylate, PEGMA - poly(ethylene glycol) dimethacrylate, SPELA - lactide-chain-extended star polyethylene glycol.

Table 5
Modeling disease models by hydrogels with vasculatures for drug screening.

Hydrogel types	Cell sources	Organoid types	Vascular morphology/signals	Major results	Ref.
GelMA, alginate	HUVECs, cardiomyocytes	Cardiac tissues	Migration of HUVECs and formation of a layer of confluent endothelium	The generation of aligned myocardium; dose-dependent responses of DOX towards HUVECs and cardiomyocytes	[49]
GelMA, PEGDA, alginate, PEGOA	MCF-7 cells, HUVECs, HLECs	Blood and lymphatic vessel pair	Perfusable blood vessels and lymphatic vessel with one blinded end	Adjusting levels of DOX diffusion using different combinations of lymphatic and blood vessels; increased IC_{50} value of DOX in 3D model	[51]
Gelatin, fibrin	ECFC-ECs, multiple tumor cell types (MCF-7, MDA-MB-231, SW620, SW480, and MNT-1)	Vascularized microtumors	Appearance of vessel-like fragments and complete networks within 3 d and 7 d, respectively	Enhanced angiogenic sprouting and vascular leakage in the vascularized microtumors with the presence of tumor cells; significant differences in IC_{50} for oxaliplatin between micro-tumors and 2D cultures	[198]
Collagen	HUVECs	Vascular sprouting	Active and rapid migration of HUVECs into hydrogel with VEGF	Diffusion of VEGF (40 ng mL^{-1}) for mimicking pro-angiogenic factors; determination of the bortezomib dosage for inhibiting the growth of vascular lumen without toxicity for HUVECs	[197]
GelMA	HUVECs, HepG2	Nonalcoholic fatty liver disease	Promotion of vascularization by coculture of nonparenchymal cells and hepatocytes	Optimization for the ratio of HepG2 and HUVECs; the maintenance of steatosis stage for more than a week; lower levels of intracellular lipids using metformin and pioglitazone after 2 d compared with the group without drugs	[177]
GelMA, alginate	HUVECs, MDA-MB-231	Breast tumor model	Elongate actin of HUVECs towards tumor cells compared with the HUVECs alone	Uniquely fabrication of microfiber-laden minispheroids; high cell viabilities of HUVECs and MDA-MB-231 cells	[120]
Collagen, gelatin	GMBs, HUVECs	Tumor tissue	Tow perfusable channels with HUVECs lining on the inner channel surface	3D GBM model *in vitro* with hollow vascular channels in the chip for long-term culture and drug delivery; decreased metabolic activity of GBM cells in 3D cell spheroids after temozolomide treatment for 21 d; the shrinkage of tumor mass	[195]

Abbreviations: 2D - two-dimension, 3D - three-dimension, DOX - doxorubicin, ECFC-ECs - human endothelial colony forming cell-derived ECs, GelMA - gelatin methacrylate, GMBs - glioblastoma multiforme cells, HepG2 - human hepatocellular carcinoma cells, HLECs - human lymphatic endothelial cells, HUVECs - human umbilical vein endothelial cells, IC_{50} - 50% inhibitory concentration, MCF-7 - human breast cancer cells, PEGDA - poly(ethylene glycol) diacrylate, PEGOA - eight-arm poly(ethylene glycol) acrylate, VEGF- vascular endothelial growth factors.

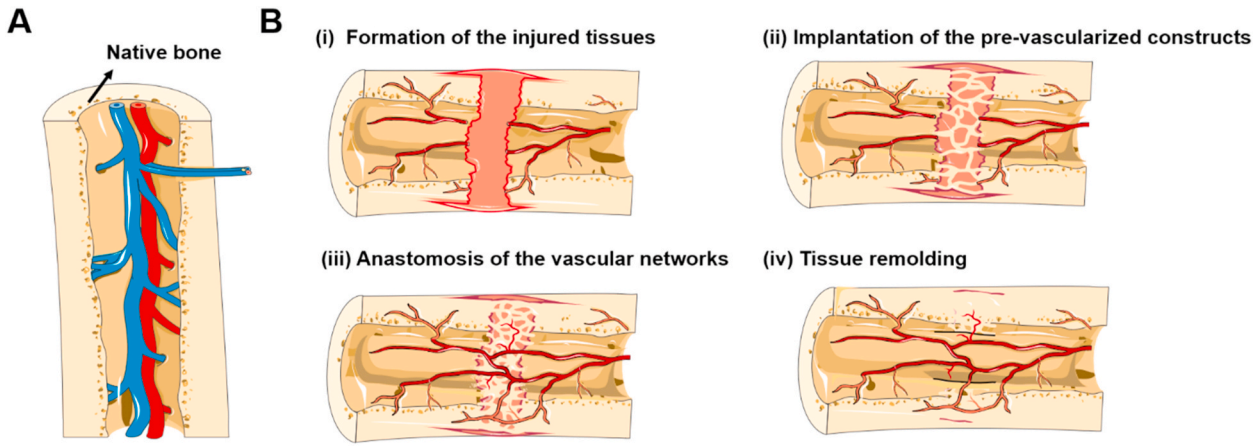

Fig. 5. Overview of the native bone tissue and bone fracture healing process. (A) Native bone is a hierarchical and heterogeneous tissue consisting of highly functional vascular networks. (B) The bone healing process upon the implantation of the pre-vascularized constructs. The repair process can be broadly classified into the following steps upon injured. (i) the recovery of injured bone tissue is usually overlooked upon severe damage due to the lack of vascular networks remolding in the defect area; (ii) the initial inflammatory phase; (iii) the subsequent regeneration phase, in which tissues and vascular systems are developed; (iv) the final tissue maturation, involving ECM remodeling and the balance between the functional achievement or scar formation.

Mitchell encapsulated HUVECs, and human adipose-derived mesenchymal stem cells (ADMSCs) within the bioactive HAMA and GelMA hydrogel [163]. The cocultured systems initially generated capillary-like networks *in vitro* and then facilitated anastomosis of these newly born capillaries with host murine vasculature upon implantation into nude mice. In addition to the involvement of various vascular cell sources and GFs, as an essential step forward, the innovative design of the perfusable microchannels within the pre-vascularized constructs is also crucial [19,33]. For example, MSCs laden GelMA hydrogel architectures with hollow microchannels were printed and implanted into the rats with femoral bone defects (Fig. 6A–i) [95]. The solid GelMA templates and the GelMA hydrogels containing rhBMP-2 as a clinically relevant dose were also implanted as negative and positive controls, respectively. Compared with these control groups, the inclusion of microchannels within GelMA architectures showed enhancing vascularization within core regions of the templates (Fig. 6A–ii). Zhang fabricated hollow-pipe-packed bioceramic scaffolds using alginate owing to the suitable viscosity and stiffness simultaneously [96]. The synergistic effect of bioactive ionic composition and the hollow pipeline structure within the scaffold facilitated early vascularization and bone regeneration *in vivo*. Cui and coworkers integrated interconnected horizontal cavity-like channels into the rigid cylindrical structures [165]. HUVEC/hMSC-laden elastic GelMA hydrogel filled these channels and maintained hollow structures using a needle-based subtractive technique, leading to the formation of the vascularized biphasic construct. Specifically, within this vascularized bone region, the angiogenic and osteogenic peptides, including VEGF peptides and BMP-2 peptides, were introduced into the corresponding regions, respectively, to accelerate both angiogenesis and osteogenesis. These interconnected vascular lumen-like channels provided an unblocked fluid environment for the unobstructed infusion of culture medium, thus enhancing the vascular invasion spaces, as well as the production of osteogenic markers. Together, these examples demonstrated that the pre-vascularization within hydrogels represented a promising approach for the regeneration of the tissues upon transplantation.

However, transplantation approaches for tissue regeneration have the disadvantages of complex surgical implantation, increasing improper adaptation to the defect site, and the risk of infections, which could sometimes cause implantation failure. By addressing these issues, the injectable vascularized hydrogels are of emerging significance in the field of tissue engineering as they can provide improved defect margin adaptation and reach the injured tissues in extreme deep places with minimum invasiveness [133]. In this vein, the risk of infection, less pain, and less scarring can be achieved upon injection. To date, according to the different shaping times and molding locations, the injectable vascularized hydrogels can be classified into molding *in vivo* after injection or pre-molding *in vitro* before injection [104].

On the one hand, as for the molding approach *in vivo*, the flowable hydrogel solution under modest pressure can fix rapidly at the target site and provide adequate integrity after injection as required [169]. In addition, due to the tunable mechanical properties and versatile biochemical cues of hydrogel pre-solution, the gel systems can be easily used as carriers for GFs, cells, and drugs [19,121,151,160,169,170]. Accordingly, the application of the injectable hydrogel towards tissue regeneration can be broad. Tang novelty developed gelatin and alginate hydrogels containing bone marrow mesenchymal stem cells (BMSCs) and atomized Mg particles simultaneously (Fig. 6C) [85]. During the gelation process after injection, H_2 gas bubbles were generated along with Mg degradation, leading to the interconnected porous structures in the hydrogel scaffolds. Moreover, the production of Mg^{2+} could further facilitate osteogenic differentiation of BMSCs. Finally, the vascularized bone regeneration was achieved with injection of this biocompatible hydrogel system after 3 weeks. In another example, Park and coworkers reported an injectable click-crosslinking HA hydrogel for bone regeneration [170]. The BMP-2 mimetic peptide was modified into the hydrogel networks, accelerating human dental pulp stem cells (hDPSCs) osteogenic differentiation *in vitro*. Moreover, after the hydrogel shaping *in vivo*, some vessels appeared on the hydrogel scaffold. Last but not least, Hu designed a reactive oxygen species (ROS)- responsive and intelligent pH-responsive injectable hydrogel by grating phenylboronic acid to the side chain of the alginate [121]. In addition, the hydrogel was effectively assembled with anti-inflammatory and antibacterial drugs using naproxen and amikacin, respectively. The positive CD31 expression of cells *in vivo* revealed the formation of newly born vessels and the acceleration of wound healing after injection.

On the other hand, in contrast to the injection of the hydrogel solution, the injection of the pre-formed vascularized hydrogel architectures before the injection is far less studied. Annamalai fabricated spheroidal fibrin-based microtissues with a diameter of 100–200 μm, embedding with human microvascular endothelial cells (HMVECs) and FBs [175]. The sprouting of HMVECs could be evidently observed within fibrin hydrogel over 7 d of culture on the 1:3 HMVECs:FBs ratio. In our previous study, we fabricated angiogenic microrods composed of alginate and gelatin harboring ECs [78]. Vascular lumen-like structures could be derived through ECs proliferation and migration. Notably, the induced angiogenesis could be observed after injection to the auricle of

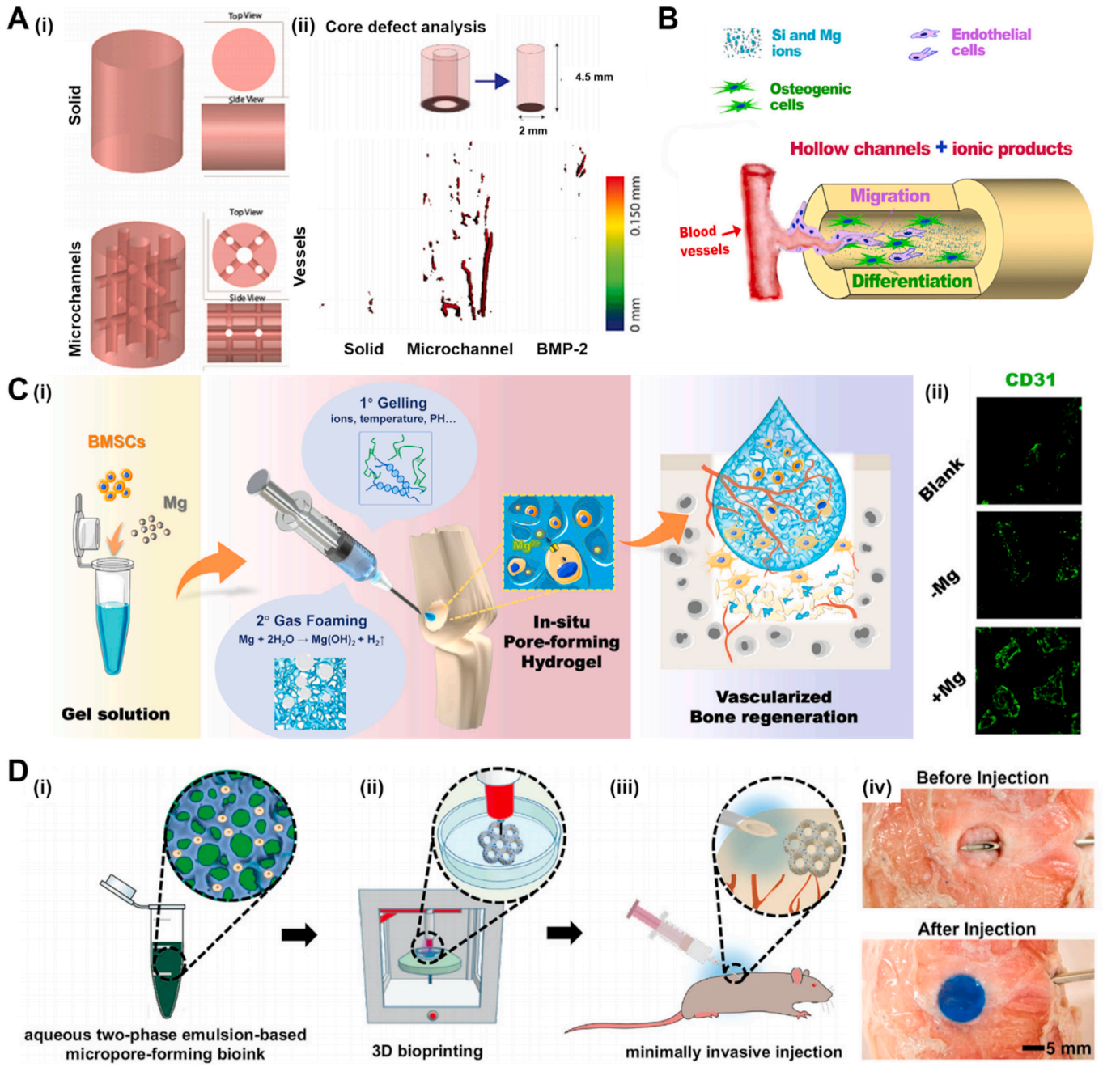

Fig. 6. (A) (i) Outline of construct design (solid and microchanneled), top and side views demonstrating interconnected microchannel network within the constructs. (ii) Casting of the anatomically shaped humeral head containing microchannels. (iii) Representative 3D reconstructions of vessel formation for each group along with corresponding 3D morphometric reconstructions of vessel diameters within the defects. Reprinted with permission from Ref. [95]. Copyright 2018, Elsevier Ltd. (B) Schematic drawing representing the printing process of the hollow-strut-packed (i.e., BRT-H) scaffolds for vascularized bone regeneration by means of the synergistic effect of the pipeline structure and bioactive ions. Reprinted with permission from Ref. [96]. Copyright 2020, Elsevier Ltd. (C) Schematic illustration. i) In summary, vascularized bone regeneration was fulfilled with the application of this direct cell-laden hydrogel, characterized by *in situ* pore-forming based on Mg degradation. (ii) The endothelial marker CD31 to visualize vascularized bone regeneration 3 weeks after defects repaired by the cell-laden porous hydrogel. Reprinted with permission from Ref. [85]. Copyright 2020, Elsevier Ltd. (D) Schematic showing the fabrication process of the 3D-bioprinted hierarchically porous hydrogel constructs by using an aqueous two-phase bioink. (i) The aqueous two-phase emulsion bioink containing the pre-gel GelMA/cell and PEO blend. (ii) 3D bioprinting and photocrosslinking. (iii)Minimally invasive injection of the hierarchically porous hydrogel constructs. (iv) Photographs showing the injectability performances using a porcine tissue model. Reprinted with permission from Ref. [84]. Copyright 2020, Wiley online library.

the SCID mice. More recently, Zhang's group developed an injectable hMSC-laden hierarchically macro-micro-nano porous GelMA hydrogel construct using 3D printing technology (Fig. 6D) [84]. Apart from the excellent cell spreading and proliferation after compression and injection, the hydrogel constructs could be designed into various sizes and shapes as defect-specific needed, enabling irregular defects repair. Since our hierarchically porous GelMA constructs could imitate the designed sites *in vivo*, the relevant vascular cell types had great potentials to be encapsulated within the construct to achieve vasculogenesis.

4.2. Organ-on-chips

Owing to the breakthrough of microfluidic techniques, the emerging organ-on-chips approach provides great opportunities for building 3D organotypic models [144]. In addition, the embedding of hydrogels within microfluidic chips is prevalent to build diverse biomimetic tissue models in terms of architectural variability, cellular fidelity, scales, and matrix composition, which enables the stimulation of physiological 3D organoids [10,49,51,144,159,171,176–181]. In this vein, remarkable progress has been made using hydrogel chips to fabricate vascular networks, replicate tissue-tissue interfaces, and reproduce parenchymal tissues.

The significant advancement of the organ-on-a-chip approach is the feasibility of growing 3D complex vessel networks on hydrogel chips. Typically, ECs are directly populated within hydrogels, which are then embedded within the microfluidic device and ultimately self-assemble into angiogenic networks [81,173]. As for this angiogenesis-on-a-chip approach, ECs sprouting, secretion of matrix proteins, the release of GFs, cellular interactions, and perivascular cell recruitments can be recapitulated and monitored to some extent within hydrogel matrixes [182,183]. For example, Kim and coworkers provided a dynamic methodology that could monitor the complex angiogenesis and vasculogenesis progress directed by ECs in response to microenvironment factors [181]. Initially, microfluidic devices were fabricated using a PDMS chip filled with fibrin gel to form an ECM microenvironment. As for the angiogenesis monitoring, the HUVECs were positioned on the side of the central channel to induce angiogenic sprouting, along with lung FBs on the opposite outside channel to form the gradient of LF-secreted factors. Additionally, the HUVECs and lung FBs were populated into the embedded 3D fibrin matrix and both outside channels, respectively, towards vasculogenesis monitoring. It was demonstrated that the vasculogenic morphogenesis of HUVECs was dependent on the presence of lung FBs, while the interconnected networks would absent without lung FBs. In another example, Jeon developed functional microvascular networks using PDMS chips composed of fibrin gel embedding with ECs and hMSCs, demonstrating that the presence of hMSCs and additional Ang-1 dictated the mean vessel diameter and number of network branches [184].

To date, in addition to the dense vessels in tissue models, numerous models directly incorporated the perfusable microchannels within chips, mimicking the 3D vascular tubular structures or endothelium barriers in native tissues [49,176,181,185]. As for this vasculogenesis-on-a-chip approach, initially, ECs surround the hollow channels to form an EC monolayer. Then, distinct cell types are populated in the multilayer chambers separately, leading to the spatial organization of various cell types, as well as compartmentalized microenvironments. In this vein, hydrogels have been widely used as cell culture substrates, compassing these endothelialized channels for enhancing permeability and organ perfusion [186,187]. For instance, a single HUVEC-lined vascular channel was embedded within FB-laden gelatin-fibrin gels in Kolesky's reports [186]. They also integrated endothelium, stroma, and parenchyma within single 3D vascularized tissues that could be directly perfused for more than 6 weeks. A significant reduction was observed in the diffusional permeability compared with gels without channels. Furthermore, as the geometry of the native vasculature varies in a wide range, these tubular structures embedded within the hydrogel matrix can be tuned in diameters. Bertassoni and colleagues embedded agarose template fibers within GelMA, PEGDMA, PEGDA, and star poly (ethylene glycol-*co*-lactide) acrylate hydrogels to create a vascular architecture [187]. After removal of the agarose template, the perfusable microchannels with diameters ranging from approximately 150 to 1000 μm could be readily fabricated. The HUVECs and MC3T3 were populated into the microchannel and hydrogel, respectively. Specifically, the formation of an endothelial monolayer on the inside of the channels and the osteogenic differentiation were confirmed.

Moreover, the interfaces between tissue-tissue could be reproduced

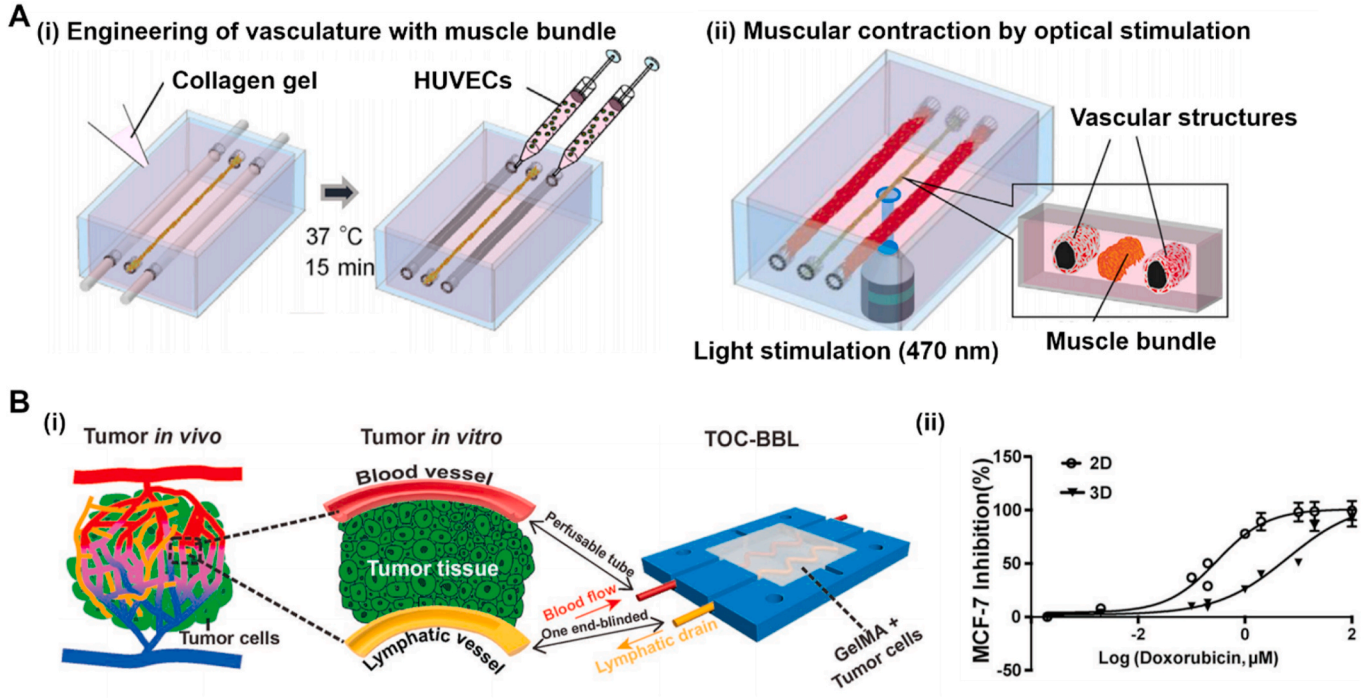

Fig. 7. (A) Schematic showing fabrication of the endothelial vessels with the muscle bundle. Reprinted with permission from Ref. [188]. Copyright 201, Elsevier Ltd. (B) (i) Schematic of the bioprinted blood and lymphatic vessel pair containing the pair of bioprinted blood/lymphatic vessel. The red-colored perfusable hollow tube was bioprinted to provide blood fluid flow, the yellow-colored one end–blinded hollow tube was bioprinted to enable lymphatic drain flow, and the chamber was seeded with tumor cells embedded in an extracellular matrix (ECM)-like a hydrogel. (ii) Dose-response curves of 2D- and 3D-cultured MCF-7 cells to DOX. Reprinted with permission from Ref. [51]. Copyright 2019, Wiley. (For interpretation of the references to color in this figure legend, the reader is referred to the Web version of this article.)

to monitor intricate interactions [10,179,180]. Osaki investigated the crosstalk between the myogenesis of mouse myoblasts (C2C12 cells) and angiogenesis of HUVECs in collagen gel (Fig. 7A) [188]. The collagen gels served as a container to support ECs sprouting, as well as the formation of filtration barrier in this model. Initially, 3D vascular structures and C2C12 muscle fiber bundles were developed within collagen gel. HUVECs exhibited angiogenic sprouting, and the robust capillary networks were formed in 5 d, which was mediated by the secretion of Ang-1 from muscle fiber bundles. Subsequently, the enhancing muscle contraction was observed due to a reciprocal response between Ang-1 and neuregulin-1 signaling that was secreted from HUVECs. Moreover, the continuous optical stimulation of muscle tissue significantly promoted angiogenic sprouting. Similarly, collagen gels were also employed to encapsulate astrocytes, along with brain ECs seeding in the apical compartment, leading to the formation of a 3D functional blood-brain barrier model [189]. As above, these vasculogenesis-like approaches are essential for enhancing pathophysiological relevance in the constructed models *in vitro*.

Nowadays, various organ-specific angiogenesis and vasculogenesis, such as ocular [171], skin [176,190], tumors [109,178], brain [94,147,191], and other endothelialized volumetric tissue models have been reported using microfluidic technology [76,192]. These target organs with complex vessels significantly enhanced the vascular delivery function, as well as the morphological complexity. Specifically, the establishment of tumor tissue units and other disease models bridge the gap between clinical trials and *in vitro* drug tests, which can be further utilized for disease studies and drug discovery in the pharmaceutical field. Moreover, we will discuss the disease hydrogel-chip for drug screening in Section 4.3.

4.3. Drug screening

The traditional assessment of drug candidates *in vitro* and *in vivo* primarily relies on the 2D cell monolayer culture on a petri dish and 3D animal models, respectively [23,193]. However, the toxicity prediction is far from accurate due to the rarely physiological microenvironment in 2D plates [159]. In addition, the ethical issues and high costs also hamper the application of animal experiments towards drug evaluation [23]. In this regard, several efforts have been dedicated to creating functional organs to accelerate the process of drug development [23,83,99,121,142,156,159,194–197]. In recent few years, hydrogel-based tissue models have garnered tremendous interest in artificial organs due to their tunable physiochemical properties, favorable permeability, and high biocompatibility [83,121,142,194,195]. Notably, such water-rich property makes it feasible to support cell growth and deliver other specific physiological and pathological triggers [99,156,197]. Moreover, the remarkable progress both in angiogenesis and vasculogenesis is transforming the field of vascular biology and its applications in drug screening [197,198]. In an example, Sobrino incorporated HUVECs with various human tumor cells as *in vitro* vascularized microtumor models [198]. Interestingly, each tumor cell line, including MCF-7 cells, melanoma cells, and human colorectal cancer cell line (SW480 and SW620), showed reproducibly different patterns of tumor growth rate, collagen synthesis, and vascular development. In addition, compared with their surrounding stroma, stronger cellular metabolism and metabolic response to various FDA-approved anti-vascular agents (pazopanib, leucovorin, vincristine, and oxaliplatin) were examined within vascularized microtumors. In another example, Kim established vascularized microtumors within collagen gel cages for screening and quantifying the VEGF-induced chemotactic response on HUVECs [197]. VEGF was explicitly added to mimic the pro-angiogenic factors secreted from the native tumor tissues. The dosage of bortezomib was determined to inhibit the growth of vascular lumen with no obvious toxicity for HUVECs.

Basically, hydrogels provide biological environments to sustain cell attachment and facilitate cell-cell interactions [99,194,196]. For instance, Ali and coworkers fabricated a non-alcoholic fatty liver disease model and demonstrated the reversibility of steatosis by antisteatotic drug administration using GelMA substrate [177]. Initially, human hepatocellular carcinoma cells (HepG2)/HUVECs cell spheroids were transferred inside GelMA hydrogel and cultured for 9 d with high viabilities. Then, the antisteatotic drugs, including metformin and pioglitazone, were introduced on the constructed nonalcoholic fatty liver disease models. The decreased level of intracellular lipids was displayed for cell spheroids after drug treatment. Typically, cell encapsulation in the hydrogel matrixes is another general approach to establish disease models. In general, cells are suspended into the hydrogel solution and then fixed in the well-defined space after the biocompatible shaping process [99,120,199]. With tumor models as an example, coculturing of tumor cells with nonparenchymal ECs can regulate metastasis of tumor cells, which is considered the most straightforward way to establish vascular functions. In an example, Xie and coworkers found that the actin of HUVECs tended to elongate towards the cocultured breast tumor cells in their GelMA tumor models by the contrast of the HUVECs alone [120]. In their fabrication process, GelMA and GelMA/alginate hydrogel solutions were extruded separately, forming a novel "microfiber-laden minispheroid" architecture. As the addition of alginate increased the liquid viscosity, ECs-laden microfibers were maintained on the surface of the MDA-MB-231-laden GelMA microbeads. Remarkably, the HUVECs tended to form a cavity and spread towards the MDA-MB-231 cells. The creative fiber-microbead architectures provided a novel cell coculture platform to study advanced antitumor drugs.

For developing more complex disease models with high tissue similarity, hydrogels are integrated within the organ-on-chip approach to generate disease models, which is similar to the other tissue models as introduced in section 4.2. However, compared with the healthy tissue models, the ability of drug delivery in the disease organ-on-chip should be taken into in-depth consideration for effective drug testing [83,99,142,156,194,195]. Indeed, PDMS, which is extremely popular as the raw material of chips, may not suitable for cellular experiments in the drug screening process. PDMS can absorb drugs or some hydrophobic molecules from infiltrating solutions, which may disturb the determination of dose-response of the drug [52–54,144]. In this vein, compared with PDMS, hydrogels with hydrophilic properties are far less drug-absorbent than PDMS [159]. Yang and coworkers designed a drug metabolism reactor using Pluronic F127-acrylamide-bisacrylamide (FAB) hydrogel that could encapsulate liver microsomes regardless of the gel concentration, while the small molecule drugs could diffuse freely [156]. Moreover, more biologically relevant to cancer can be attained using hydrogel-based disease chips. For example, in Zhang's group, microcirculation systems compromising lymphatic and blood vessels were established within the tumor masses for drug screening (Fig. 7B–i) [51]. Specifically, the one end-blinded hollow lymph vessel and perfusable blood vessel were fabricated using PEGDA/alginate/-GelMA and eight-arm poly (ethylene glycol) acrylate (PEGOA)/alginate/GelMA inks, respectively, with tunable permeability profiles mimicking their native counterparts. Subsequently, the lymph and blood vessels were embedded in GelMA matrixes compromising MCF-7 cells to conduct DOX delivery. The significantly higher 50% inhibitory concentration (IC_{50}) values of DOX were observed in 3D cultured-MCF-7 cells than 2D-cultured cells (Fig. 7B–ii). Moreover, the potential effects of the cell on DOX delivery were investigated by seeding human lymphatic endothelial cells (HLECs) and HUVECs onto the surfaces of the lymphatic and blood vessels, respectively. The slower diffusion rates compared with the group without cells demonstrated that the endothelial layers and barriers were formed due to the tight cell junctions, indicating more biologically relevance. In another instance, Ozturk integrated gelatin channels into the collagen layers, leading to the establishment of a 3D glioblastoma multiforme model (GBM) with perfusable vascular channels [195]. Gelatin was used as a sacrificial material for the creation of two fluidic vascular channels on the top of collagen layers. HUVECs were then seeded on the inner channel surface to format

a cell lining. Consequently, the 3D GBM cell spheroids (>400 μm) suspended in collagen showed a significant decrease in metabolic activity level than 2D cell monolayer after 21 d of temozolomide treatment. Above all, hydrogels can be integrated into customizable *in vitro* disease models effectively, thus providing more therapeutic options with enhanced physiological settings for predicting drug efficacy.

5. Conclusions and future trends

In this review, we have overviewed the significant advances in hydrogels for generating endothelialized and vascularized tissue constructs. With the help of the near-physiological microenvironment, the constructed 3D tissue models with vasculature have presented impressive applications in tissue regeneration, vascular biology, drug screening, and other regenerative medicine fields. However, there are still some challenges that should be considered for more preclinical and clinical applications.

The bottom-up tissue engineering approach involves cell types, scaffold materials, and GFs. In this vein, the source of cells, design of suitable hydrogels, and profile of angiogenic factors should be carefully considered, respectively. To date, an extensive of tissue models have verified the necessity of HUVECs for vasculature [50,78,126,137,139]. Unfortunately, HUVECs have shown poor adult cellular markers due to their fetal umbilical cord origin. Besides that, the ECs from the aorta artery are not suitable to investigate embryonic angiogenesis [98]. In this case, the sources of ECs should be taken into consideration since their phenotypes should match with the organotypic features to prevent invalid researches. Moreover, as the patient-derived ECs are regarded as the most reliable cell sources, the standard and reproducible protocols for ECs isolation and derivation should be tackled urgently in order to mimic organ-specific situations. An equally bothering problem that should be addressed is the collaboration between cells and scaffolds. Regardless of the synthetic or natural sources, the hydrogel matrixes provide biocompatible surroundings for achieving cell functions and morphogenesis during the formation of vascularized organoids. Although the viscosity, functional signals, and hybrid parts of hydrogel pre-solution are diverse and tunable, the cell differentiation influenced by each factor is still obscure and confusing. Furthermore, as for the solid hydrogel, it seems the cell activities, such as cell spreading, immigration, proliferation, and self-organization, are closely related to the mechanical properties of hydrogel after shaping. However, it is still far less studied about the impact of reduced mechanical strength and swollen volume on vascularization and tissue formation in the long-term culture period. Above all, the limited reciprocate interactions between cells and scaffolds hamper the simulation of angiogenesis or vasculogenesis in the native tissue or organs. In addition, on the molecular scale, the integration of GFs or GF-mimetic proteins into the hydrogel matrixes enables the formation of functionality and physicochemical properties resembling the *in vivo* circulatory routes. However, most of the current GF-delivery strategies in hydrogel systems are insufficient in mimicking physiological homeostasis. While the lifespan of the GFs can be extended to some extent, the precise release profile and accurate dose control are currently unavailable.

With the help of more sophisticated engineering techniques in the last few years, the development of vascularized tissue constructs based on hydrogel has made great progress. The role of prevalent and efficient techniques, including but not limited to 3D printing, microfluidics, electric spinning, and molding approaches, are essential in engineering meso- or microvasculature. Also, these advancing technologies cannot be ignored for shaping vascularized tissue constructs. Nevertheless, manufacturing a 3D vascular network is still challenging due to the bare integration of tubular hydrogel architectures and branched vascular networks. Actually, the vascular tress with a wide range of diameter distributes the entire body. Therefore, depending on the application of the vascularized tissue constructs, 3D architectures with structural complexity are still required. In addition, while some efforts have been paid to improve equipment accuracy for higher resolution, the shear stress during extrusion within equipment and overwhelming force during hydrogel curing may decrease dispersed cell viabilities. Furthermore, the evaluation of cell functions and the formation of vascularized tissue constructs *via* live imaging face even more challenges. Besides more technical requirements, corresponding characterizations for cell activities and cell functions also have much room for improvement. To date, the size of the engineered 3D tissue models ranges from millimeters to centimeters. In this case, the prevalent fluorescence imaging techniques have difficulties in capturing these largely constructed architectures due to the limited field of view. The finite shallow depth penetration also hampers the imaging process. Although sometimes the samples can be observed in bright fields, the increased cell number and altering in the morphology of the hydrogel can blur the field of vision after long-term culture. Hence, further efforts are required to ameliorate engineering techniques and capturing approaches.

By far, few of the vascularized tissue models have translated into the clinic successfully. Actually, the extent of vascularization in the engineered constructs is far less compared with the natural counterparts. Especially for transplantation, transplant surgery is extremely complicated for most parts of organs and tissue defects. In addition, the artificially suturing between host vessels and perfusable structures is unrealistic for hydrogel materials due to insufficient mechanical strength. Although angiogenesis and vasculogenesis can be detected to some extent, the vascular anastomosis between the vascularization in the implant and the host vasculature is far less studied. Consequently, in-depth comprehension and realization of this integration are necessary for the survival of the implant after grafting and the restoration of tissue function after a period of convalescence. Moreover, despite recent developments in angiogenesis/vasculogenesis on-a-chip have solved some physiological phenomena such as vascular sprouting and anastomosis, these customized chips *in vitro* sometimes fail to consider the interaction of multiple organs and the regulation of the dynamic microenvironment *in vivo*. Accordingly, a multi-organs-on-a-chip with vasculature seems better for enhancing physiologically relevant organ-organ linking. Especially in some disease models, this multi-organ-chip approach would allow more complex vascularized orthotopic models to substitute animal models for drug screening. Overall, with further optimization investigation in this field, the continuous outcoming of vascularized tissues with better patient compliance will surely board the application in regeneration medicine.

CRediT authorship contribution statement

Ying Wang: Conceptualization, Writing - original draft. **Ranjith Kumar Kankala:** Writing - original draft, Validation. **Caiwen Ou:** Funding acquisition. **Aizheng Chen:** Supervision, Funding acquisition, Project administration. **Zhi-Lu Yang:** Supervision, Project administration.

Declaration of competing interest

The authors declare no potential conflicts of interest with this work.

Acknowledgment

This study received financial support from the High-level Talents Research and Development Program of Affiliated Dongguan Hospital, Southern Medical University (K202102), National Natural Science Foundation of China (NSFC, 81971734, 31771099, 81871504), National Key R&D Program of China (2019YFE0113600), and Program for Innovative Research Team in Science and Technology in Fujian Province.

References

[1] K.H. Hussein, K.M. Park, L. Yu, S.H. Song, H.M. Woo, H.H. Kwak, Vascular reconstruction: a major challenge in developing a functional whole solid organ graft from decellularized organs, Acta Biomater. 103 (2020) 68–80.

[2] B.X. Wang, X.G. Lv, Z. Li, M.H. Zhang, J.J. Yao, N. Sheng, M.J. Lu, H.P. Wang, S. Y. Chen, Urethra-inspired biomimetic scaffold: a therapeutic strategy to promote angiogenesis for urethral regeneration in a rabbit model, Acta Biomater. 102 (2020) 247–258.

[3] J. Lee, D.Y. Park, Y.J. Seo, J.J. Chung, Y.M. Jung, S.H. Kim, Organ-level functional 3D tissue constructs with complex compartments and their preclinical applications, Adv. Mater. 32 (51) (2020) 2002096.

[4] S.Y. Tan, Z.W. Leung, A.R. Wu, Recreating physiological environments in vitro: design rules for microfluidic-based vascularized tissue constructs, Small 16 (9) (2020) 1905055.

[5] N. Ashammakhi, M.A. Darabi, S. Kehr, A. Erdem, S. Hu, M. Dokmeci, A. Nasr, A. Khademhosseini, Advances in controlled oxygen generating biomaterials for tissue engineering and regenerative therapy, Biomacromolecules 21 (1) (2020) 56–72.

[6] G.D. Yancopoulos, S. Davis, N.W. Gale, J.S. Rudge, J. Holash, Vascular-specific growth factors and blood vessel formation, Nature 407 (6801) (2000) 242–248.

[7] M.A. Schwartz, D. Vestweber, M. Simons, A unifying concept in vascular health and disease, Science 360 (6386) (2018) 270–271.

[8] C. Betsholtz, Transcriptional control of endothelial energy, Nature 529 (7585) (2016) 160–161.

[9] J. Folkman, C. Haudenschild, Angiogenesis in vitro, Nature 288 (5791) (1980) 551–556.

[10] R.K. Kankala, S.B. Wang, A.Z. Chen, Microengineered organ-on-a-chip platforms towards personalized medicine, Curr. Pharmaceut. Des. 24 (45) (2018) 5354–5366.

[11] S. Yin, W.J. Zhang, Z.Y. Zhang, X.Q. Jiang, Recent advances in scaffold design and material for vascularized tissue-engineered bone regeneration, Adv. Healthcare Mater. 8 (10) (2019), e1801433.

[12] I. Redenski, S. Guo, M. Machour, A. Szklanny, S. Landau, B. Kaplan, R.I. Lock, Y. Gabet, D. Egozi, G. Vunjak-Novakovic, S. Levenberg, Engineered vascularized flaps, composed of polymeric soft tissue and live bone, repair complex tibial defects, Adv. Funct. Mater. (2021) 2008687.

[13] W.W. Cho, B.S. Kim, M.J. Ahn, Y.H. Ryu, D.H. Ha, J.S. Kong, J.W. Rhie, D.W. Cho, Flexible adipose-vascular tissue assembly using combinational 3D printing for volume-stable soft tissue reconstruction, Adv. Healthcare Mater. 10 (6) (2020) 2001693.

[14] G.A. Primo, A. Mata, 3D Patterning within hydrogels for the recreation of functional biological environments, Adv. Funct. Mater. 31 (16) (2021) 2009574.

[15] M.d.M. Ferrà Cañellas, M. Munar Bestard, L. Garcia Sureda, B. Lejeune, J. M. Ramis, M. Monjo, BMP4 micro-immunotherapy increases collagen deposition and reduces PGE2 release in human gingival fibroblasts and increases tissue viability of engineered 3D gingiva under inflammatory conditions, J. Periodontol. (2021) 1–12.

[16] X.Z. Wang, Z. Chen, B.B. Zhou, X.Y. Duan, W.J. Weng, K. Cheng, H.M. Wang, J. Lin, Cell-sheet-derived ECM coatings and their effects on BMSCs responses, ACS Appl. Mater. Interfaces 10 (14) (2018) 11508–11518.

[17] S. Chameettachal, D. Prasad, Y. Parekh, S. Basu, V. Singh, K.K. Bokara, F. Pati, Prevention of corneal myofibroblastic differentiation in vitro using a biomimetic ECM hydrogel for corneal tissue regeneration, ACS Appl. Bio Mater. 4 (1) (2021) 533–544.

[18] Z.L. Yang, X. Zhao, R. Hao, Q.F. Tu, X.H. Tian, Y. Xiao, K.Q. Xiong, M. Wang, Y. H. Feng, N. Huang, G.Q. Pan, Bioclickable and mussel adhesive peptide mimics for engineering vascular stent surfaces, Proc. Natl. Acad. Sci. Unit. States Am. 117 (28) (2020) 16127.

[19] J. Lee, K.Y. Lee, Local and sustained vascular endothelial growth factor delivery for angiogenesis using an injectable system, Pharm. Res. (N. Y.) 26 (7) (2009) 1739–1744.

[20] S. Lu, J. Lam, J.E. Trachtenberg, E.J. Lee, H. Seyednejad, J.J.J.P. van den Beucken, Y. Tabata, M.E. Wong, J.A. Jansen, A.G. Mikos, F.K. Kasper, Dual growth factor delivery from bilayered, biodegradable hydrogel composites for spatially-guided osteochondral tissue repair, Biomaterials 35 (31) (2014) 8829–8839.

[21] J. Saremi, M. Khanmohammadi, M. Azami, J. Ai, A. Yousefi-Ahmadipour, S. Ebrahimi-Barough, Tissue-engineered nerve graft using silk-fibroin/polycaprolactone fibrous mats decorated with bioactive cerium oxide nanoparticles, J. Biomed. Mater. Res. (2021) 1–11.

[22] C.J. Chang, A. Taniguchi, Establishment of a nanopatterned renal disease model by mimicking the physical and chemical cues of a diseased mesangial cell microenvironment, ACS Appl. Bio Mater. 4 (2) (2021) 1573–1583.

[23] Y. Wang, R.K. Kankala, J.T. Zhang, L.Z. Hao, K. Zhu, S.B. Wang, Y.S. Zhang, A. Z. Chen, Modeling endothelialized hepatic tumor microtissues for drug screening, Adv. Sci. 7 (21) (2020) 2002002.

[24] R.K. Kankala, J. Zhao, C.G. Liu, X.J. Song, D.Y. Yang, K. Zhu, S.B. Wang, Y. S. Zhang, A.Z. Chen, Highly porous microcarriers for minimally invasive in situ skeletal muscle cell delivery, Small 15 (25) (2019) 1901397.

[25] Y.J. Seo, S. Jeong, J.J. Chung, S.H. Kim, N. Choi, Y. Jung, Development of an anisotropically organized brain dECM hydrogel-based 3D neuronal culture platform for recapitulating the brain microenvironment in vivo, ACS Biomater. Sci. Eng. 6 (1) (2020) 610–620.

[26] H. Lee, W. Kim, J. Lee, J.J. Yoo, G.H. Kim, S.J. Lee, Effect of hierarchical scaffold consisting of aligned dECM nanofibers and poly(lactide-co-glycolide) struts on the orientation and maturation of human muscle progenitor cells, ACS Appl. Mater. Interfaces 11 (43) (2019) 39449–39458.

[27] H. Yu, S.X. Yu, H. Qiu, P. Gao, Y.Z. Chen, X. Zhao, Q.F. Tu, M.G. Zhou, L. Cai, N. Huang, K.Q. Xiong, Z.L. Yang, Nitric oxide-generating compound and bio-clickable peptide mimic for synergistically tailoring surface anti-thrombogenic and anti-microbial dual-functions, Bioact. Mater. 6 (6) (2021) 1618–1627.

[28] B.S. Kim, S. Das, J. Jang, D.W. Cho, Decellularized extracellular matrix-based bioinks for engineering tissue- and organ-specific microenvironments, Chem. Rev. 120 (19) (2020) 10608–10661.

[29] G.D. Kusuma, M.C. Yang, S.P. Brennecke, A.J. O'Connor, B. Kalionis, D.E. Heath, Transferable matrixes produced from decellularized extracellular matrix promote proliferation and osteogenic differentiation of mesenchymal stem cells and facilitate Scale-Up, ACS Biomater. Sci. Eng. 4 (5) (2018) 1760–1769.

[30] H. Nokhbatolfoghahaei, Z. Paknejad, M. Bohlouli, M. Rezai Rad, P. Aminishakib, S. Derakhshan, L. Mohammadi Amirabad, N. Nadjmi, A. Khojasteh, Fabrication of decellularized engineered extracellular matrix through bioreactor-based environment for bone tissue engineering, ACS Omega 5 (49) (2020) 31943–31956.

[31] T. Yang, Z.Y. Du, H. Qiu, P. Gao, X. Zhao, H.Y. Wang, Q.F. Tu, K.Q. Xiong, N. Huang, Z.L. Yang, From surface to bulk modification: plasma polymerization of amine-bearing coating by synergic strategy of biomolecule grafting and nitric oxide loading, Bioact. Mater. 5 (1) (2020) 17–25.

[32] X.Y. Li, J.X. Liu, T. Yang, H. Qiu, L. Lu, Q.F. Tu, K.Q. Xiong, N. Huang, Z.L. Yang, Mussel-inspired "built-up" surface chemistry for combining nitric oxide catalytic and vascular cell selective properties, Biomaterials 241 (2020) 119904.

[33] B.M. Baker, B. Trappmann, S.C. Stapleton, E. Toro, C.S. Chen, Microfluidics embedded within extracellular matrix to define vascular architectures and pattern diffusive gradients, Lab Chip 13 (16) (2013) 3246–3252.

[34] S. Park, H. Yuk, R. Zhao, Y.S. Yim, E.W. Woldeghebriel, J. Kang, A. Canales, Y. Fink, G.B. Choi, X. Zhao, P. Anikeeva, Adaptive and multifunctional hydrogel hybrid probes for long-term sensing and modulation of neural activity, Nat. Commun. 12 (1) (2021) 3435.

[35] T.-C. Tang, E. Tham, X. Liu, K. Yehl, A.J. Rovner, H. Yuk, C. de la Fuente-Nunez, F.J. Isaacs, X. Zhao, T.K. Lu, Hydrogel-based biocontainment of bacteria for continuous sensing and computation, Nat. Chem. Biol. 17 (6) (2021) 724–731.

[36] J. Zhang, Y. Zheng, J. Lee, J. Hua, S. Li, A. Panchamukhi, J. Yue, X. Gou, Z. Xia, L. Zhu, X. Wu, A pulsatile release platform based on photo-induced imine-crosslinking hydrogel promotes scarless wound healing, Nat. Commun. 12 (1) (2021) 1670.

[37] D. Zhu, Z. Li, K. Huang, T.G. Caranasos, J.S. Rossi, K. Cheng, Minimally invasive delivery of therapeutic agents by hydrogel injection into the pericardial cavity for cardiac repair, Nat. Commun. 12 (1) (2021) 1412.

[38] Q.L. Zhu, C. Du, Y. Dai, M. Daab, M. Matejdes, J. Breu, W. Hong, Q. Zheng, Z. L. Wu, Light-steered locomotion of muscle-like hydrogel by self-coordinated shape change and friction modulation, Nat. Commun. 11 (1) (2020) 5166.

[39] O. Wichterle, D. Lím, Hydrophilic gels for biological use, Nature 185 (4706) (1960) 117–118.

[40] F. Lim, A.M. Sun, Microencapsulated islets as bioartificial endocrine pancreas, Science 210 (4472) (1980) 908–910.

[41] W. Shi, J. Huang, R.C. Fang, M.J. Liu, Imparting functionality to the hydrogel by magnetic-field-induced nano-assembly and macro-response, ACS Appl. Mater. Interfaces 12 (5) (2020) 5177–5194.

[42] J. Kopecek, Hydrogel biomaterials: a smart future, Biomaterials 28 (34) (2007) 5185–5192.

[43] F.Y. Hsieh, H.W. Han, X.R. Chen, C.S. Yang, Y. Wei, S.H. Hsu, Non-viral delivery of an optogenetic tool into cells with self-healing hydrogel, Biomaterials 174 (2018) 31–40.

[44] A.T. Young, O.C. White, M.A. Daniele, Rheological properties of coordinated physical gelation and chemical crosslinking in gelatin methacryloyl (GelMA) hydrogels, Macromol. Biosci. 20 (12) (2020) 2000183.

[45] L.D. Zhang, S.M. Liang, Y.Q. Tu, Q. Chen, W.W. Han, Microscopical hollow hydrogel springs, necklaces and ladders: a tubular microbot as a potential vascular scavenger, Mater. Horiz. 6 (10) (2019) 2135–2142.

[46] Y.P. Liu, P.D. Xu, Z. Liang, R.X. Xie, M.Y. Ding, H.X. Liu, Q.L. Liang, Hydrogel microfibers with perfusable folded channels for tissue constructs with folded morphology, RSC Adv. 8 (42) (2018) 23475–23480.

[47] C.D. Ley, M.W.B. Olsen, E.L. Lund, P.E.G. Kristjansen, Angiogenic synergy of bFGF and VEGF is antagonized by Angiopoietin-2 in a modified in vivo matrigel assay, Microvasc. Res. 68 (3) (2004) 161–168.

[48] S. Fleischer, D.N. Tavakol, G. Vunjak-Novakovic, From arteries to capillaries: approaches to engineering human vasculature, Adv. Funct. Mater. 30 (37) (2020) 1910811.

[49] Y.S. Zhang, A. Arneri, S. Bersini, S.-R. Shin, K. Zhu, Z. Goli-Malekabadi, J. Aleman, C. Colosi, F. Busignani, V. Dell'Erba, C. Bishop, T. Shupe, D. Demarchi, M. Moretti, M. Rasponi, M.R. Dokmeci, A. Atala, A. Khademhosseini, Bioprinting 3D microfibrous scaffolds for engineering endothelialized myocardium and heart-on-a-chip, Biomaterials 110 (2016) 45–59.

[50] Y. Wang, R.K. Kankala, K. Zhu, S.B. Wang, Y.S. Zhang, A.Z. Chen, Coaxial extrusion of tubular tissue constructs using a gelatin/GelMA blend bioink, ACS Biomater. Sci. Eng. 5 (10) (2019) 5514–5524.

[51] X. Cao, R. Ashfaq, F. Cheng, S. Maharjan, J. Li, G.L. Ying, S. Hassan, H.Y. Xiao, K. Yue, Y.S. Zhang, A tumor-on-a-chip system with bioprinted blood and lymphatic vessel pair, Adv. Funct. Mater. 29 (31) (2019) 1807173.

[52] A.K. Gupta, J.M. Coburn, J. Davis-Knowlton, E. Kimmerling, D.L. Kaplan, L. Oxburgh, Scaffolding kidney organoids on silk, J. Tissue Eng. Regen. Med. 13 (5) (2019) 812–822.

[53] P.K. Gavel, H.S. Parmar, V. Tripathi, N. Kumar, A. Biswas, A.K. Das, Investigations of anti-inflammatory activity of a peptide-based hydrogel using rat air pouch model, ACS Appl. Mater. Interfaces 11 (3) (2019) 2849–2859.
[54] R.J. Nagao, J. Xu, P. Luo, J. Xue, Y. Wang, S. Kotha, W. Zeng, X.Y. Fu, J. Himmelfarb, Y. Zheng, Decellularized human kidney cortex hydrogels enhance kidney microvascular endothelial cell maturation and quiescence, Tissue Eng. 22 (19–20) (2016) 1140–1150.
[55] B. Wang, W.W. Li, D. Dean, M.K. Mishra, K.S. Wekesa, Enhanced hepatogenic differentiation of bone marrow derived mesenchymal stem cells on liver ECM hydrogel, J. Biomed. Mater. Res. 106 (3) (2018) 829–838.
[56] M. Saheli, M. Sepantafar, B. Pournasr, Z. Farzaneh, M. Vosough, A. Piryaei, H. Baharvand, Three-dimensional liver-derived extracellular matrix hydrogel promotes liver organoids function, J. Cell. Biochem. 119 (6) (2018) 4320–4333.
[57] R. Randriantsilefisoa, Y. Hou, Y.W. Pan, J.L.C. Camacho, M.W. Kulka, J.G. Zhang, R. Haag, Interaction of human mesenchymal stem cells with soft nanocomposite hydrogels based on polyethylene glycol and dendritic polyglycerol, Adv. Funct. Mater. 30 (1) (2020) 1905200.
[58] W.M. Han, M. Mohiuddin, S.E. Anderson, A.J. García, Y. Jang, Co-delivery of Wnt7a and muscle stem cells using synthetic bioadhesive hydrogel enhances murine muscle regeneration and cell migration during engraftment, Acta Biomater. 94 (2019) 243–252.
[59] T. Distler, A. Sulistio, D. Schneidereit, O. Friedrich, R. Detsch, A.R. Boccaccini, 3D printed oxidized alginate-gelatin bioink provides guidance for C2C12 muscle precursor cell orientation and differentiation via shear stress during bioprinting, Biofabrication 12 (4) (2020), 045005.
[60] Y.J. Choi, Y.J. Jun, D.Y. Kim, H.G. Yi, S.H. Chae, J.S. Kang, J.Y. Lee, G. Gao, J. S. Kong, J. Jang, A 3D cell printed muscle construct with tissue-derived bioink for the treatment of volumetric muscle loss, Biomaterials 206 (2019) 160–169.
[61] P. Pushp, R. Bhaskar, S. Kelkar, N. Sharma, D. Pathak, M.K. Gupta, Plasticized poly(vinylalcohol) and poly(vinylpyrrolidone) based patches with tunable mechanical properties for cardiac tissue engineering applications, Biotechnol. Bioeng. 118 (6) (2021) 2312–2325.
[62] T. Su, K. Huang, M.A. Daniele, M.T. Hensley, A.T. Young, J. Tang, T.A. Allen, A. C. Vandergriff, P.D. Erb, F.S. Ligler, K. Cheng, Cardiac stem cell patch integrated with microengineered blood vessels promotes cardiomyocyte proliferation and neovascularization after acute myocardial infarction, ACS Appl. Mater. Interfaces 10 (39) (2018) 33088–33096.
[63] W.J. Kim, G.H. Kim, Intestinal villi model with blood capillaries fabricated using collagen-based bioink and dual-cell-printing process, ACS Appl. Mater. Interfaces 10 (48) (2018) 41185–41196.
[64] S.Y. Tan, Z. Leung, A.R. Wu, Recreating physiological environments in vitro: design rules for microfluidic based vascularized tissue constructs, Small 16 (9) (2020) 1905055.
[65] H. Saman, S.S. Raza, S. Uddin, K. Rasul, Inducing angiogenesis, a key step in cancer vascularization, and treatment approaches, Cancers 12 (5) (2020) 1172.
[66] S. Negri, P. Faris, R. Berra-Romani, G. Guerra, F. Moccia, Endothelial transient receptor potential channels and vascular remodeling: extracellular Ca^{2+} entry for angiogenesis, arteriogenesis and vasculogenesis, Front. Physiol. 10 (2020) 1618.
[67] L. Elomaa, Y.P. Yang, Additive manufacturing of vascular grafts and vascularized tissue constructs, Tissue Eng. B Rev. 23 (5) (2017) 436–450.
[68] M.W. Laschke, M.D. Menger, Vascularization in tissue engineering: angiogenesis versus inosculation, Eur. Surg. Res. 48 (2) (2012) 85–92.
[69] Y.J. Blinder, A. Freiman, N. Raindel, D.J. Mooney, S. Levenberg, Vasculogenic dynamics in 3D engineered tissue constructs, Sci. Rep. 5 (1) (2015) 17840.
[70] V. Wu, M.N. Helder, N. Bravenboer, C.M. ten Bruggenkate, J. Jin, J. Klein-Nulend, E.A.J.M. Schulten, Bone tissue regeneration in the oral and maxillofacial region: a review on the application of stem cells and new strategies to improve vascularization, Stem Cell. Int. 30 (2019) 6279721.
[71] D. Sharma, D. Ross, G.F. Wang, W.K. Jia, S. Kirkpatrick, F. Zhao, Upgrading prevascularization in tissue engineering: a review of strategies for promoting highly organized microvascular network formation, Acta Biomater. 1 (95) (2019) 112–130.
[72] M.W. Laschke, M.D. Menger, Prevascularization in tissue engineering: current concepts and future directions, Biotechnol. Adv. 34 (2) (2015) 112–121.
[73] N. Conkling, S. WIsel, G. Faleo, T. Desai, Q.Z. Tang, Prevascularization of the subcutaneous space improves survival of transplanted mouse islets, Transplantation 102 (2018) S372.
[74] D. Gholobova, L. Terrie, M. Gerard, H. Declercq, L. Thorrez, Vascularization of tissue-engineered skeletal muscle constructs, Biomaterials 235 (2019) 119708.
[75] L.L. Ouyang, J.P.K. Armstrong, Q. Chen, Y.Y. Lin, M.M. Stevens, Void-free 3D bioprinting for in situ endothelialization and microfluidic perfusion, Adv. Funct. Mater. 30 (1) (2020) 1908349.
[76] T. Sun, Q. Shi, Q. Liang, Y.B. Yao, H.P. Wang, J.Z. Sun, Q. Huang, T. Fukuda, Fabrication of vascular smooth muscle-like tissues based on self-organization of circumferentially aligned cells in microengineered hydrogels, Lab Chip 20 (17) (2020) 3120–3131.
[77] L. Wang, L.X. Zhu, Z. Wang, A.J. Lou, Y.X. Yang, Y. Guo, S. Liu, C. Zhang, Z. Zhang, H.S. Hu, B. Yang, P. Zhang, H.W. Ouyang, Z.Y. Zhang, Development of a centrally vascularized tissue engineering bone graft with the unique core-shell composite structure for large femoral bone defect treatment, Biomaterials 175 (2018) 44–60.
[78] Y. Wang, X. Hu, R.K. Kankala, D.Y. Yang, K. Zhu, S.B. Wang, Y.S. Zhang, A. Z. Chen, Endothelialized microrods for minimally invasive in situ neovascularization, Biofabrication 12 (1) (2020), 015011.
[79] Y.J. Wu, V.D. Ranjan, Y.L. Zhang, A living 3D in vitro neuronal network cultured inside hollow electrospun microfibers, Adv. Biosys. 2 (5) (2018) 1700218.
[80] J.M. Zhu, P. He, L. Lin, D.R. Jones, R.E. Marchant, Biomimetic poly(ethylene glycol)-based hydrogels as scaffolds for inducing endothelial adhesion and capillary-like network formation, Biomacromolecules 13 (3) (2012) 706–713.
[81] V.V. Duinen, D. Zhu, C. Ramakers, A.J.V. Zonneveld, P. Vulto, T. Hankemeier, Perfused 3D angiogenic sprouting in a high-throughput in vitro platform, Angiogenesis 22 (2019) 157–165.
[82] P.Q. Meng, S. Maharjan, X. Yan, X. Liu, B. Singh, A.M.v. Genderen, F. Robledo-Padilla, R. Parra-Saldivar, N. Hu, W.T. Jia, C.L. Xu, J. Kang, S. Hassan, C. Hai Bo, X. Hou, A. Khademhosseini, Y.S. Zhang, Digitally tunable microfluidic bioprinting of multilayered cannular tissues, Adv. Mater. 30 (2017) 1706913.
[83] X. Song, Z.X. Zhang, J.L. Zhu, Y.T. Wen, F. Zhao, L.J. Lei, N. Phan-Thien, B. C. Khoo, J. Li, Thermoresponsive hydrogel induced by dual supramolecular assemblies and its controlled release property for enhanced anticancer drug delivery, Biomacromolecules 21 (4) (2021) 1516–1527.
[84] G.L. Ying, N. Jiang, C. Parra-Cantu, G.S. Tang, J.Y. Zhang, H.J. Wang, S.X. Chen, N.P. Huang, J.W. Xie, Y.S. Zhang, Bioprinted injectable hierarchically porous gelatin methacryloyl hydrogel constructs with shape-memory properties, Adv. Funct. Mater. 30 (2020) 2003740.
[85] Y.M. Tang, S.H. Lin, S. Yin, F. Jiang, M.L. Zhou, G.Z. Yang, N.J. Sun, W.J. Zhang, X.Q. Jiang, In situ gas foaming based on magnesium particle degradation: a novel approach to fabricate injectable macroporous hydrogels, Biomaterials 232 (2020) 119727.
[86] G.L. Ying, N. Jiang, S. Maharjan, Y.X. Yin, R.R. Chai, X. Cao, J.Z. Yang, A.K. Miri, S. Hassan, Y.S. Zhang, Aqueous two-phase emulsion bioink-enabled 3D bioprinting of porous hydrogels, Adv. Mater. 30 (50) (2018), e1805460.
[87] Z.F. Wang, G. An, Y. Zhu, X.M. Liu, Y.H. Chen, H.K. Wu, Y.J. Wang, X.T. Shi, C. B. Mao, 3D-printable self-healing and mechanically reinforced hydrogels with host–guest non-covalent interactions integrated into covalently linked networks, Mater. Horiz. 6 (4) (2019) 733–742.
[88] S. Trujillo, S.L. Vega, K.H. Song, A.S. Félix, M.J. Dalby, J.A. Burdick, M. Salmeron-Sanchez, Engineered full-length fibronectin-hyaluronic acid hydrogels for stem cell engineering, Adv. Healthcare Mater. 9 (21) (2020) 2000989.
[89] Q.F. Liang, F. Gao, Z.W. Zeng, J.R. Yang, M.M. Wu, C.J. Gao, D.L. Cheng, H. B. Pan, W.G. Liu, C.S. Ruan, Coaxial scale-up printing of diameter-tunable biohybrid hydrogel microtubes with high strength, perfusability, and endothelialization, Adv. Funct. Mater. 30 (43) (2020) 2001485.
[90] M.T. S, B.Y. C, O. A, D.K. H, S.M. L, H.J. K, J.S. R, J.S. L, H. H, Y.J. L, Reinforced-hydrogel encapsulated hMSCs towards brain injury treatment by trans-septal approach, Biomaterials 266 (2021) 120413.
[91] B. Natan, K. Hanjun, J.G. Marcus, L. KangJu, B. Praveen, A.B. Ethan, S. Einollah, S. Wujin, Z. Shiming, C. Hyun-Jong, C.H. Martin, O. Serge, A. Samad, H. Saber, A. Nureddin, R.D. Mehmet, H. Rondinelli Donizetti, L. Junmin, K. Ali, Biofabrication of endothelial cell, dermal fibroblast, and multilayered keratinocyte layers for skin tissue engineering, Biofabrication 13 (3) (2020), 035030.
[92] L. Xu, M. Varkey, A. Jorgensen, J.H. Ju, Q.H. Jin, J.H. Park, Y. Fu, G.L. Zhang, D. X. Ke, W.X. Zhao, R.X. Hou, A. Atala, Bioprinting small diameter blood vessel constructs with an endothelial and smooth muscle cell bilayer in a single step, Biofabrication 12 (4) (2020), 045012.
[93] J.R. Tse, A.J. Engler, Preparation of hydrogel substrates with tunable mechanical properties, Current Protocols in Cell Biology 47 (1) (2010), 10.16.1-10.16.16.
[94] C. Marco, S. Yoojin, O. Tatsuya, H. Cynthia, C. Valeria, R.D. Kamm, 3D self-organized microvascular model of the human blood-brain barrier with endothelial cells, pericytes and astrocytes, Biomaterials 180 (2018) 117–129.
[95] A.C. Daly, P. Pitacco, J. Nulty, G.M. Cunniffe, D.J. Kelly, 3D printed microchannel networks to direct vascularisation during endochondral bone repair, Biomaterials 162 (2018) 34–46.
[96] W.J. Zhang, C. Feng, G.Z. Yang, G.L. Li, X. Ding, S.Y. Wang, Y.D. Dou, Z.Y. Zhang, J. Chang, C.T. Wu, X.Q. Jiang, 3D-printed scaffolds with synergistic effect of hollow-pipe structure and bioactive ions for vascularized bone regeneration, Biomaterials 135 (2017) 85–95.
[97] C. Nica, Z.K. Lin, A. Sculean, M.B. Asparuhova, Adsorption and release of growth factors from four different porcine-derived collagen matrices, Materials 13 (11) (2020) 2635.
[98] A.J. Minor, K.L.K. Coulombe, Engineering a collagen matrix for cell-instructive regenerative angiogenesis, J. Biomed. Mater. Res. 108 (6) (2020) 2407–2416.
[99] D. Yip, C.H. Cho, A multicellular 3D heterospheroid model of liver tumor and stromal cells in collagen gel for anti-cancer drug testing, Biochem. Biophys. Res. Commun. 433 (3) (2013) 327–332.
[100] G.H. Kim, S. Ahn, Y.Y. Kim, Y. Cho, W. Chun, Coaxial structured collagen-alginate scaffolds: fabrication, physical properties, and biomedical application for skin tissue regeneration, J. Mater. Chem. 21 (17) (2011) 6165–6172.
[101] G. Eke, N. Mangir, N. Hasirci, S. Macneil, V. Hasirci, Development of a UV crosslinked biodegradable hydrogel containing adipose derived stem cells to promote vascularization for skin wounds and tissue engineering, Biomaterials 129 (2017) 188–198.
[102] Y.N. Zhang, R.K. Avery, Q. Vallmajo-Martin, A. Assmann, A. Vegh, A. Memic, B. D. Olsen, N. Annabi, A. Khademhosseini, A highly elastic and rapidly crosslinkable elastin-like polypeptide-based hydrogel for biomedical applications, Adv. Funct. Mater. 25 (30) (2015) 4814–4826.
[103] F. Wu, Y. Pang, J.Y. Liu, Swelling-strengthening hydrogels by embedding with deformable nanobarriers, Nat. Commun. 11 (1) (2020) 4502.
[104] S. Yasmeen, M.K. Lo, S. Bajracharya, M. Roldo, Injectable scaffolds for bone regeneration, Langmuir 30 (43) (2014) 12977–12985.

[105] S.R. Shin, H. Bae, J.M. Cha, J.Y. Mun, Y.C. Chen, H. Tekin, H. Shin, S. Farshchi, M. R. Dokmeci, S. Tang, A. Khademhosseini, Carbon nanotube reinforced hybrid microgels as scaffold materials for cell encapsulation, ACS Nano 6 (1) (2012) 362–372.
[106] J. Park, J. Jeon, B. Kim, M.S. Lee, S. Park, J. Lim, J. Yi, H. Lee, H.S. Yang, J.Y. Lee, Electrically conductive hydrogel nerve guidance conduits for peripheral nerve regeneration, Adv. Funct. Mater. 30 (39) (2020) 2003759.
[107] T.W. Xin, Y. Gu, R.Y. Cheng, J.C. Tang, Z.Y. Sun, W.G. Cui, L. Chen, Inorganic strengthened hydrogel membrane as regenerative periosteum, ACS Appl. Mater. Interfaces 9 (47) (2017) 41168–41180.
[108] M. Miyazaki, T. Maeda, K. Hirashima, N. Kurokawa, K. Nagahama, A. Hotta, PEG-based nanocomposite hydrogel: thermoresponsive sol-gel transition controlled by PLGA-PEG-PLGA molecular weight and solute concentration, Polymer 115 (2017) 246–254.
[109] S. Lee, S. Kim, D.J. Koo, J. Yu, H. Cho, H. Lee, J.M. Song, S.Y. Kim, D.H. Min, N. L. Jeon, 3D microfluidic platform and tumor vascular mapping for evaluating anti-angiogenic RNAi-based nanomedicine, ACS Nano 15 (1) (2021) 338–350.
[110] H.X. Hu, L.L. Dong, Z.H. Bu, Y.F. Shen, J. Luo, H. Zhang, S.C. Zhao, F. Lv, Z.T. Liu, miR-23a-3p-abundant small extracellular vesicles released from Gelma/nanoclay hydrogel for cartilage regeneration, J. Extracell. Vesicles 9 (1) (2020) 1778883.
[111] I. Jahan, E. George, N. Saxena, S. Sen, Silver-nanoparticle-entrapped soft GelMA gels as prospective scaffolds for wound healing, ACS Appl. Bio Mater. 2 (5) (2019) 1802–1814.
[112] A.K. Gaharwar, N.A. Peppas, A. Khademhosseini, Nanocomposite hydrogels for biomedical applications, Biotechnol. Bioeng. 111 (3) (2014) 441–453.
[113] H.L. Zhu, X.Y. Li, M.J. Yuan, W.G. Wan, M.Y. Hu, X.D. Wang, X.J. Jiang, Intramyocardial delivery of bFGF with a biodegradable and thermosensitive hydrogel improves angiogenesis and cardioprotection in infarcted myocardium, Exp. Ther. Med. 14 (2017) 3609–3615.
[114] Y.M. An, L.M. Gao, T.Y. Wang, Graphene oxide/alginate hydrogel fibers with hierarchically arranged helical structures for soft actuator application, ACS Appl. Nano Mater. 3 (6) (2020) 5079–5087.
[115] H.W. Ooi, C. Mota, A.T. ten Cate, A. Calore, L. Moroni, M.B. Baker, Thiol-ene alginate hydrogels as versatile bioinks for bioprinting, Biomacromolecules 19 (8) (2018) 3390–3400.
[116] C. Lee, J. Shin, J.S. Lee, E. Byun, J.H. Ryu, S.H. Um, D. Kim, H. Lee, S.W. Cho, Bioinspired, calcium-free alginate hydrogels with tunable physical and mechanical properties and improved biocompatibility, Biomacromolecules 14 (6) (2013) 2004–2013.
[117] J.M. Zhu, Bioactive modification of poly(ethylene glycol) hydrogels for tissue engineering, Biomaterials 31 (17) (2010) 4639–4656.
[118] Y. Hong, F.F. Zhou, Y.J. Hua, X.Z. Zhang, C.Y. Ni, D.H. Pan, Y.Q. Zhang, D. M. Jiang, L. Yang, Q.N. Lin, Y.W. Zou, D.S. Yu, D.E. Arnot, X.H. Zou, L.Y. Zhu, S. F. Zhang, H.W. Ouyang, A strongly adhesive hemostatic hydrogel for the repair of arterial and heart bleeds, Nat. Commun. 10 (1) (2019) 2060.
[119] N. Zhou, X. Ma, K.V. Bernaerts, P. Ren, W. Hu, T. Zhang, Expansion of oarian cancer stem-like cells in poly(ethylene glycol)-cross-linked poly(methyl vinyl ether-alt-maleic acid) and alginate double-network hydrogels, ACS Biomater. Sci. Eng. 6 (6) (2020) 3310–3326.
[120] M. Xie, Q. Gao, J. Qiu, J. Fu, Z. Chen, Y. He, 3D biofabrication of microfiber-laden minispheroids: a facile 3D cell co-culturing system, Biomater. Sci. 8 (1) (2020) 109–117.
[121] C. Hu, F.J. Zhang, L.Y. Long, Q.S. Kong, R.F. Luo, Y.B. Wang, Dual-responsive injectable hydrogels encapsulating drug-loaded micelles for on-demand antimicrobial activity and accelerated wound healing, J. Contr. Release 324 (2020) 204–217.
[122] Y.Y. Sun, C. Chen, X.X. Zhang, W. Shi, R.H. Zhu, A.H. Zhou, S.J. Chen, J.H. Feng, Heparin improves alveolarization and vascular development in hyperoxia-induced bronchopulmonary dysplasia by inhibiting neutrophil extracellular traps, Biochem. Biophys. Res. Commun. 522 (1) (2020) 33–39.
[123] J.A. Whisler, M.B. Chen, R.D. Kamm, Control of perfusable microvascular network morphology using a multiculture microfluidic system, Tissue Eng. C Methods 20 (7) (2014) 543–552.
[124] R. Haubner, W. Schmitt, G. Holzemann, S.L. Goodman, A. Jonczyk, H. Kessler, Cyclic RGD peptides containing β-turn mimetics, J. Am. Chem. Soc. 118 (34) (1996) 7881–7891.
[125] E. Locardi, D.G. Mullen, R.H. Mattern, M. Goodman, Conformations and pharmacophores of cyclic RGD containing peptides which selectively bind integrin alpha(v)beta 3, J. Pept. Sci. 5 (11) (1999) 491–506.
[126] H. Lee, Y.C. Jin, S.W. Kim, I.-D. Kim, H.K. Lee, J.K. Lee, Proangiogenic functions of an RGD-SLAY-containing osteopontin icosamer peptide in HUVECs and in the postischemic brain, Exp. Mol. Med. 50 (1) (2018) e430.
[127] K.C. Franz, C.V. Suschek, V. Grotheer, M. Akbas, N. Pallua, Impact of growth factor content on proliferation of mesenchymal stromal cells derived from adipose tissue, PloS One 15 (4) (2020), e0230265.
[128] X.Z. Wan, P.F. Li, X.X. Jin, F. Su, J. Shen, J. Yuan, Poly(ε-caprolactone)/keratin/heparin/VEGF biocomposite mats for vascular tissue engineering, J. Biomed. Mater. Res. 108 (2) (2020) 292–300.
[129] J. Zhu, C. Tang, K. Kottke Marchant, R.E. Marchant, Design and synthesis of biomimetic hydrogel scaffolds with controlled organization of cyclic RGD peptides, Bioconjugate Chem. 20 (2) (2009) 333–339.
[130] C.M. Chen, J.C. Tang, Y. Gu, L.L. Liu, X.Z. Liu, L.F. Deng, C. Martins, B. Sarmento, W.G. Cui, L. Chen, Bioinspired hydrogel electrospun fibers for spinal cord regeneration, Adv. Funct. Mater. 29 (4) (2019) 1806899.
[131] H. Shirahama, B.H. Lee, L.P. Tan, N.J. Cho, Precise tuning of facile one-pot gelatin methacryloyl (GelMA) synthesis, Sci. Rep. 6 (1) (2016) 31036.
[132] Y. Jun, M.L. Yan, Y.C. Wang, J.Z. Fu, H.R. Suo, 3D bioprinting of low-concentration cell-laden gelatin methacrylate (GelMA) bioinks with a two-step cross-linking strategy, ACS Appl. Mater. Interfaces 10 (8) (2018) 6849–6857.
[133] S. Bak, T. Ahmad, Y.B. Lee, J.Y. Lee, H. Shin, Delivery of a cell patch of cocultured endothelial cells and smooth muscle cells using thermoresponsive hydrogels for enhanced angiogenesis, Tissue Eng. 22 (1–2) (2016) 182–193.
[134] J.E. Leslie Barbick, J.J. Moon, J.L. West, Covalently-immobilized vascular endothelial growth factor promotes endothelial cell tubulogenesis in poly (ethylene glycol) diacrylate hydrogels, J. Biomater. Sci. Polym. Ed. 20 (12) (2009) 1763–1779.
[135] D. Barati, S.R.P. Shariati, S. Moeinzadeh, M. Martin, A. Khademhosseini, E. Jabbari, Spatiotemporal release of BMP-2 and VEGF enhances osteogenic and vasculogenic differentiation of human mesenchymal stem cells and endothelial colony-forming cells co-encapsulated in a patterned hydrogel, J. Contr. Release 223 (2016) 126–136.
[136] G. An, F.X. Guo, X.M. Liu, Z.F. Wang, Y. Zhu, Y. Fan, C.K. Xuan, Y. Li, H.K. Wu, X. T. Shi, C.B. Mao, Functional reconstruction of injured corpus cavernosa using 3D-printed hydrogel scaffolds seeded with HIF-1α-expressing stem cells, Nat. Commum. 11 (1) (2020) 2687.
[137] W.T. Jia, P.S. Gungor-Ozkerim, Y.S. Zhang, K. Yue, W.J. Liu, Q.M. Pi, B. Byambaa, M.R. Dokmeci, S.R. Shin, A. Khademhosseini, Direct 3D bioprinting of perfusable vascular constructs using a blend bioink, Biomaterials 106 (2016) 58–68.
[138] S.L. Faley, E.H. Neal, J.X. Wang, A.M. Bosworth, C.M. Weber, K.M. Balotin, E. S. Lippmann, L.M. Bellan, iPSC-derived brain endothelium exhibits stable, long-term barrier function in perfused hydrogel scaffolds, Stem Cell Rep 12 (3) (2019) 474–487.
[139] J.A. Li, K. Zhang, Y. Xu, J. Chen, P. Yang, Y.C. Zhao, A. Zhao, N. Huang, A novel coculture model of HUVECs and HUASMCs by hyaluronic acid micropattern on titanium surface, J. Biomed. Mater. Res. 102 (6) (2014) 1950–1960.
[140] L. Klee, Specifics of EPC and EPCM, International Construction Contract Law (2015) 66–87.
[141] Y.G. Cui, S.L. Fu, D. Sun, J.C. Xing, T.Y. Hou, X.H. Wu, EPC-derived exosomes promote osteoclastogenesis through LncRNA-MALAT1, J. Cell Mol. Med. 23 (6) (2019) 3843–3854.
[142] K. Hida, N. Maishi, K. Akiyama, H. Ohmura Kakutani, C. Torii, N. Ohga, T. Osawa, H. Kikuchi, H. Morimoto, M. Morimoto, M. Shindoh, N. Shinohara, Y. Hida, Tumor endothelial cells with high aldehyde dehydrogenase activity show drug resistance, Canc. Sci. 108 (11) (2017) 2195–2203.
[143] B. Natan, K. Hanjun, J.G. Marcus, L. KangJu, B. Praveen, A.B. Ethan, S. Einollah, S. Wujin, Z. Shiming, C. Hyun-Jong, C.H. Martin, O. Serge, A. Samad, H. Saber, A. Nureddin, R.D. Mehmet, H. Rondinelli Donizetti, L. Junmin, K. Ali, Biofabrication of endothelial cell, dermal fibroblast, and multilayered keratinocyte layers for skin tissue engineering, Biofabrication 13 (3) (2020), 035030.
[144] H.T. Liu, Y.Q. Wang, K.L. Cui, Y.Q. Guo, J.H. Qin, Advances in hydrogels in organoids and organs-on-a-chip, Adv. Mater. 31 (50) (2019) 1902042.
[145] C.C. Wang, Y. Abu-Amer, R.J. O'Keefe, J. Shen, Loss of dnmt3b in chondrocytes leads to delayed endochondral ossification and fracture repair, J. Bone Miner. Res. 33 (2) (2018) 283–297.
[146] D. Taniguchi, K. Matsumoto, R. Machino, Y. Takeoka, A. Elgalad, Y. Taura, S. Oyama, T. Tetsuo, M. Moriyama, K. Takagi, M. Kunizaki, T. Tsuchiya, T. Miyazaki, G. Hatachi, N. Matsuo, K. Nakayama, T. Nagayasu, Human lung microvascular endothelial cells as potential alternatives to human umbilical vein endothelial cells in bio-3D-printed trachea-like structures, Tissue Cell 63 (2020) 101321.
[147] R. Reskiawan, M.M. Alwjwaj, O.A. Othman, K. Rakkar, U. Bayraktutan, Outgrowth endothelial cells form a functional cerebral barrier and restore its integrity after damage, Neural Regen. Res. 15 (6) (2020) 1071–1078.
[148] C.A. DeForest, K.S. Anseth, Cytocompatible click-based hydrogels with dynamically tunable properties through orthogonal photoconjugation and photocleavage reactions, Nat. Chem. 3 (12) (2011) 925–931.
[149] N. Yonet-Tanyeri, M.H. Rich, M. Lee, M.H. Lai, J.H. Jeong, R.J. Devolder, H. Kong, The spatiotemporal control of erosion and molecular release from micropatterned poly(ethylene glycol)-based hydrogel, Biomaterials 34 (33) (2013) 8416–8423.
[150] D.H.R. Kempen, L. Lu, A. Heijink, T.E. Hefferan, L.B. Creemers, A. Maran, M. J. Yaszemski, W.J.A. Dhert, Effect of local sequential VEGF and BMP-2 delivery on ectopic and orthotopic bone regeneration, Biomaterials 30 (14) (2009) 2816–2825.
[151] J.C. Rose, M. Cámara-Torres, K. Rahimi, J. Köhler, M. Möller, L. De Laporte, Nerve cells decide to orient inside an injectable hydrogel with minimal structural guidance, Nano Lett. 17 (6) (2017) 3782–3791.
[152] Y.S. Zhang, A. Khademhosseini, Advances in engineering hydrogels, Science 356 (6337) (2017), eaaf3627.
[153] S. Uman, A. Dhand, J.A. Burdick, Recent advances in shear-thinning and self-healing hydrogels for biomedical applications, J. Appl. Polym. Sci. 137 (25) (2020) 48668.
[154] W.K. Hu, Z.J. Wang, Y. Xiao, S.M. Zhang, J.L. Wang, Advances in crosslinking strategies of biomedical hydrogels, Biomater. Sci. 7 (3) (2019) 843–855.
[155] Y.L. Tsai, P. Theato, C.F. Huang, S.H. Hsu, A 3D-printable, glucose-sensitive and thermoresponsive hydrogel as sacrificial materials for constructs with vascular-like channels, Appl. Mater. Today 20 (7) (2020) 100778.
[156] H.Y. Yang, Y.T. Zheng, B. Zhao, T.F. Shao, Q.L. Shi, N. Zhou, W.M. Cai, Encapsulation of liver microsomes into a thermosensitive hydrogel for characterization of drug metabolism and toxicity, Biomaterials 34 (38) (2013) 9770–9778.

[157] X.M. Sun, Q. Lang, H.B. Zhang, L.Y. Cheng, Y. Zhang, G.Q. Pan, X. Zhao, H. L. Yang, Y.G. Zhang, H.A. Santos, W.G. Cui, Electrospun photocrosslinkable hydrogel fibrous scaffolds for rapid in vivo vascularized skin flap regeneration, Adv. Funct. Mater. 27 (2) (2017) 1604617.
[158] R.Z. Lin, Y.C. Chen, R. Moreno Luna, A. Khademhosseini, J.M. Melero Martin, Transdermal regulation of vascular network bioengineering using a photopolymerizable methacrylated gelatin hydrogel, Biomaterials 34 (28) (2013) 6785–6796.
[159] J.H. Zhu, Application of organ-on-chip in drug discovery, J. Biosci. Med. 8 (3) (2020) 119–134.
[160] X.L. Hou, X. Dai, J. Yang, B. Zhang, D.H. Zhao, C.Q. Li, Z.Y. Yin, Y.D. Zhao, B. Liu, Injectable polypeptide-engineered hydrogel depot for amplifying the anti-tumor immune effect induced by chemo-photothermal therapy, J. Mater. Chem. B 8 (37) (2020) 8623–8633.
[161] H.N. He, C.J. Yang, F. Wang, Z. Wei, J.L. Shen, D. Chen, C.H. Fan, H.J. Zhang, K. Liu, Mechanically strong globular protein-based fibers via microfluidic spinning technique, Angew. Chem. Int. Ed. 59 (11) (2019) 4344–4348.
[162] S. Wüst, M.E. Godla, R. Müller, S. Hofmann, Tunable hydrogel composite with two-step processing in combination with innovative hardware upgrade for cell-based three-dimensional bioprinting, Acta Biomater. 10 (2) (2014) 630–640.
[163] M.A. Kuss, S.H. Wu, Y. Wang, J.B. Untrauer, W.L. Li, J.Y. Lim, B. Duan, Prevascularization of 3D printed bone scaffolds by bioactive hydrogels and cell co-culture, J. Biomed. Mater. Res. B Appl. Biomater. 160 (5) (2017) 1788–1798.
[164] D.B. Kolesky, R.L. Truby, A.S. Gladman, T.A. Busbee, K.A. H, J.A. Lewis, 3D bioprinting of vascularized, heterogeneous cell-laden tissue constructs, Adv. Mater. 26 (19) (2014) 3124–3130.
[165] H.T. Cui, W. Zhu, M. Nowicki, X. Zhou, A. Khademhosseini, L.G. Zhang, Hierarchical fabrication of engineered vascularized bone biphasic constructs via dual 3D bioprinting: integrating regional bioactive factors into architectural design, Adv. Healthcare Mater. 5 (17) (2016) 2174–2181.
[166] S.B. Gutekunst, K. Siemsen, S. Huth, A. Mhring, B. Hesseler, M. Timmermann, I. Paulowicz, Y.K. Mishra, L. Siebert, R. Adelung, 3D hydrogels containing interconnected microchannels of subcellular size for capturing human pathogenic acanthamoeba castellanii, ACS Biomater. Sci. Eng. 5 (4) (2019) 1784–1792.
[167] M.H. Ge, J.J. Sun, M.L. Chen, J.J. Tian, H.C. Yin, J. Yin, A hyaluronic acid fluorescent hydrogel based on fluorescence resonance energy transfer for sensitive detection of hyaluronidase, Anal. Bioanal. Chem. 412 (2020) 1915–1923.
[168] Z.J. He, H.X. Zang, L. Zhu, K. Huang, T.L. Yi, S. Zhang, S.X. Cheng, An anti-inflammatory peptide and brain-derived neurotrophic factor-modified hyaluronan-methylcellulose hydrogel promotes nerve regeneration in rats with spinal cord injury, Int. J. Nanomed. 14 (2019) 721–732.
[169] N. Pettinelli, S. Rodríguez-Llamazares, R. Bouza, L. Barral, S. Feijoo-Bandín, F. Lago, Carrageenan-based physically crosslinked injectable hydrogel for wound healing and tissue repairing applications, Int. J. Pharm. 589 (2020) 119828.
[170] S.H. Park, J.Y. Park, Y.B. Ji, H.J. Ju, B.H. Min, M.S. Kim, An injectable click-crosslinked hyaluronic acid hydrogel modified with a BMP-2 mimetic peptide as a bone tissue engineering scaffold, Acta Biomater. 117 (2020) 108–120.
[171] J. Ko, Y. Lee, S. Lee, S.R. Lee, N.L. Jeon, Angiogenesis: human ocular angiogenesis-inspired vascular models on an injection-molded microfluidic chip, Adv. Healthcare Mater. 8 (15) (2019) 1970063.
[172] G.L. Ying, N. Jiang, C. Parra Cantu, G.S. Tang, J.Y. Zhang, H.J. Wang, S.X. Chen, N.P. Huang, J.W. Xie, Y.S. Zhang, Bioprinted injectable hierarchically porous gelatin methacryloyl hydrogel constructs with shape-memory properties, Adv. Funct. Mater. 30 (2020) 2003740.
[173] S.K. Ramasamy, A.P. Kusumbe, L. Wang, R.H. Adams, Endothelial Notch activity promotes angiogenesis and osteogenesis in bone, Nature 507 (2014), 376-280.
[174] Y. Zhang, Y. Liu, Z. Jiang, J. Wang, Z. Xu, K. Meng, H. Zhao, Poly(glyceryl sebacate)/silk fibroin small-diameter artificial blood vessels with good elasticity and compliance, Smart Materials in Medicine 2 (2021) 74–86.
[175] R. Tiruvannamalai Annamalai, A.Y. Rioja, A.J. Putnam, J.P. Stegemann, Vascular network formation by human microvascular endothelial cells in modular fibrin microtissues, ACS Biomater. Sci. Eng. 2 (11) (2016) 1914–1925.
[176] B.S. Kwak, S.-P. Jin, S.J. Kim, E.J. Kim, J.H. Chung, J.H. Sung, Microfluidic skin chip with vasculature for recapitulating the immune response of the skin tissue, Biotechnol. Bioeng. 117 (6) (2020) 1853–1863.
[177] S. Lasli, H.-J. Kim, K. Lee, C.-A.E. Suurmond, M. Goudie, P. Bandaru, W. Sun, S. Zhang, N. Zhang, S. Ahadian, M.R. Dokmeci, J. Lee, A. Khademhosseini, Liver-on-a-chip: a human liver-on-a-chip platform for modeling nonalcoholic fatty liver disease, Adv. Biosys. 3 (8) (2019) 1970084.
[178] J. Ko, J. Ahn, S. Kim, Y. Lee, J. Lee, D. Park, N.L. Jeon, Tumor spheroid-on-a-chip: a standardized microfluidic culture platform for investigating tumor angiogenesis, Lab Chip 19 (17) (2019) 2822–2833.
[179] S. Lasli, H.-J. Kim, K. Lee, C.-A.E. Suurmond, M. Goudie, P. Bandaru, W.J. Sun, S. M. Zhang, N.Y. Zhang, S. Ahadian, M.R. Dokmeci, J. Lee, A. Khademhosseini, A human liver-on-a-chip platform for modeling nonalcoholic fatty liver disease, Adv. Biosys. 3 (2019) 1900104.
[180] S.Z. Yu, A. Arneri, S. Bersini, S.R. Shin, A. Khademhosseini, Bioprinting 3D microfibrous scaffolds for engineering endothelialized myocardium and heart-on-a-chip, Biomaterials 110 (2016) 45–59.
[181] S. Kim, H. Lee, M. Chung, N.L. Jeon, Engineering of functional, perfusable 3D microvascular networks on a chip, Lab Chip 13 (8) (2013) 1489–1500.
[182] C. Hu, Y.F. Chen, M.J.A. Tan, K.N. Ren, H.K. Wu, Microfluidic technologies for vasculature biomimicry, Analyst 144 (15) (2019) 4461–4471.
[183] C.G.M. van Dijk, M.M. Brandt, N. Poulis, J. Anten, M. van der Moolen, L. Kramer, E.F.G.A. Homburg, L. Louzao-Martinez, J. Pei, M.M. Krebber, B.W.M. van Balkom, P. de Graaf, D.J. Duncker, M.C. Verhaar, R. Luttge, C. Cheng, A new microfluidic model that allows monitoring of complex vascular structures and cell interactions in a 3D biological matrix, Lab Chip 20 (10) (2020) 1827–1844.
[184] J.S. Jeon, B. Simone, J.A. Whisler, M.B. Chen, D. Gabriele, J.L. Charest, M. Matteo, R.D. Kamm, Generation of 3D functional microvascular networks with human mesenchymal stem cells in microfluidic systems, Integr. Biol. 6 (5) (2014) 555–563.
[185] Y. Hou, X. Deng, C. Xie, Biomaterial surface modification for underwater adhesion, Smart Materials in Medicine 1 (2020) 77–91.
[186] D.B. Kolesky, K.A. Homan, M.A. Skylar Scott, J.A. Lewis, Three-dimensional bioprinting of thick vascularized tissues, Proc. Natl. Acad. Sci. Unit. States Am. 113 (12) (2016) 3179–3184.
[187] L.E. Bertassoni, M. Cecconi, V. Manoharan, M. Nikkhah, J. Hjortnaes, A. L. Cristino, G. Barabaschi, D. Demarchi, M.R. Dokmeci, Y. Yang, A. Khademhosseini, Hydrogel bioprinted microchannel networks for vascularization of tissue engineering constructs, Lab Chip 14 (13) (2014) 2202–2211.
[188] T. Osaki, V. Sivathanu, R.D. Kamm, Crosstalk between developing vasculature and optogenetically engineered skeletal muscle improves muscle contraction and angiogenesis, Biomaterials 156 (2018) 65–76.
[189] K.L. Sellgren, B.T. Hawkins, S. Grego, An optically transparent membrane supports shear stress studies in a three-dimensional microfluidic neurovascular unit model, Biomicrofluidics 9 (6) (2015), 061102.
[190] N. Jusoh, J. Ko, N.L. Jeon, Microfluidics-based skin irritation test using in vitro 3D angiogenesis platform, APL Bioeng 3 (3) (2019), 036101.
[191] S. Lee, M. Chung, S.R. Lee, N.L. Jeon, 3D brain angiogenesis model to reconstitute functional human blood-brain barrier in vitro, Biotechnol. Bioeng. 117 (3) (2020) 748–762.
[192] J.F. Wong, M.D. Mohan, E.W.K. Young, C.A. Simmons, Integrated electrochemical measurement of endothelial permeability in a 3D hydrogel-based microfluidic vascular model, Biosens. Bioelectron. 147 (2020) 111757.
[193] X. Zhang, G. Chen, Y. Yu, L. Sun, Y. Zhao, Bioinspired adhesive and antibacterial microneedles for versatile transdermal drug delivery, Research 2020 (2020) 3672120.
[194] Y.L. Wang, J.Y. Wang, Mixed hydrogel bead-based tumor spheroid formation and anticancer drug testing, Analyst 139 (10) (2014) 2449–2458.
[195] M. Ozturk, V. Lee, H.Y. Zou, R. Friedel, G.H. Dai, X. Intes, High-resolution tomographic analysis of in vitro 3D glioblastoma tumor model under long-term drug treatment, Sci. Adv. 6 (10) (2020), eaay7513.
[196] F.F. Fu, L.R. Shang, F.Y. Zheng, Z.Y. Chen, H. Wang, J. Wang, Z.Z. Gu, Y.J. Zhao, Cells cultured on core-shell photonic crystal barcodes for drug screening, ACS Appl. Mater. Interfaces 8 (22) (2016) 13840–13848.
[197] C. Kim, J. Kasuya, J. Jeon, S. Chung, R.D. Kamm, A quantitative microfluidic angiogenesis screen for studying anti-angiogenic therapeutic drugs, Lab Chip 15 (1) (2014) 301–310.
[198] A. Sobrino, D.T.T. Phan, R. Datta, X.L. Wang, S.J. Hachey, M. Romero López, E. Gratton, A.P. Lee, S.C. George, C.C.W. Hughes, 3D microtumors in vitro supported by perfused vascular networks, Sci. Rep. 6 (1) (2016) 31589.
[199] G. Chen, Y. Yu, X. Wu, G. Wang, G. Gu, F. Wang, J. Ren, H. Zhang, Y. Zhao, Microfluidic electrospray niacin metal-organic frameworks encapsulated microcapsules for wound healing, Research 2019 (2019) 6175398.
[200] R. Tamura, M. Fujioka, Y. Morimoto, K. Ohara, K. Kosugi, Y. Oishi, M. Sato, R. Ueda, H. Fujiwara, T. Hikichi, S. Noji, N. Oishi, K. Ogawa, Y. Kawakami, T. Ohira, K. Yoshida, M. Toda, A VEGF receptor vaccine demonstrates preliminary efficacy in neurofibromatosis type 2, Nat. Commun. 10 (1) (2019) 5758.
[201] K. Tsukamoto, N. Shinzawa, A. Kawai, M. Suzuki, H. Kidoya, N. Takakura, H. Yamaguchi, T. Kameyama, H. Inagaki, H. Kurahashi, Y. Horiguchi, Y. Doi, The Bartonella autotransporter BafA activates the host VEGF pathway to drive angiogenesis, Nat. Commun. 11 (1) (2020) 3571.
[202] S.P. Zhu, Y.B. Yang, Y. He, X.X. Zhong, J.H. Ye, Z.Y. Huang, M. Chen, Q.J. Wu, Y. F. Zhang, Z.Y. Xiang, Y.R. Tu, W.Y. Ying, J. Xiao, X.K. Li, Q.S. Ye, Z.G. Wang, Hypoxia response element-directed expression of bFGF in dental pulp stem cells improve the hypoxic environment by targeting pericytes in SCI rats, Bioact. Mater. 6 (8) (2021) 2452–2466.
[203] L. Kurmann, M. Okoniewski, O.O. Ogunshola, B. Leeners, R.K. Dubey, Transcryptomic analysis of human brain microvascular endothelial response to-pericytes: cell orientation defines barrier function, Cells 10 (4) (2021) 963.